Elastic and inelastic local strain fields in composites with coated fibers or particles: theory and validation

George Chatzigeorgiou
LEM3-UMR 7239 CNRS, France

Fodil Meraghni
LEM3-UMR 7239 CNRS, France

Received 6 September 2018; accepted 10 December 2018

Abstract
This paper deals with mean field multiscale approaches for coated fiber- or particle-reinforced composites under nonlinear strain. The current work attempts to extend Dvorak's well-known transformation field analysis for mean field approaches, in which the composite's constitutive law is split into an elastic and an inelastic part. The classical Eshelby's inhomogeneity problem considering eigenstrains is revisited in order to address the presence of a coating layer. For this scope, three different methodologies are employed, one for general ellipsoidal inhomogeneities, a modified composite cylinder method for long cylindrical fibers and a modified composite sphere method for spherical particles. After identifying proper interaction tensors for the inhomogeneity and its coating layer, the composite's overall response is evaluated by extending classical mean field techniques, such as the Mori–Tanaka and the self-consistent methods. Numerical examples illustrate the differences in macroscopic and microscopic predictions between the general approach and the modified composite cylinder and sphere Assemblages.

Keywords
Mean field methods, composite cylinder assemblage, composite sphere assemblage, transformation field analysis, inelastic interaction tensors

1. Introduction

The explosion in the usage of composites in many engineering sectors (mechanical, electrical, civil engineering, aerospace, biomechanics, etc.) have created excessive demands on experimental and modeling strategies that account for the microstructural characteristics of these materials. Moreover, the requirements of modern applications very often lead to design composite structures that operate in regimes where nonlinear dissipative mechanisms occur. These effects necessitate the development of multiscale computational tools that take into account nonlinear deformation processes and damage-related phenomena.

During the last 40 years, a plethora of homogenization models has been proposed in the literature to study the local and global nonlinear response of composites [1–4]. The most popular approaches for composites with random microstructures are the so-called mean field methods [5–7], which are based on

Corresponding author:
George Chatzigeorgiou, LEM3-UMR 7239 CNRS, Arts et Métiers ParisTech, 4 Rue Augustin Fresnel 57078 Metz, France.
Email: georges.chatzigeorgiou@ensam.eu

Eshelby's well-known equivalence principle [8]. The advantage of these methods is that they provide analytical or semi-analytical formulas, which drastically reduce the computational cost. Computational strategies using the Mori–Tanaka, self-consistent, and similar types of method have been developed to study composites undergoing viscoelastic, elastoplastic, viscoplastic, or damaged mechanisms [9–24].

An important factor for correctly identifying the overall response of the composite is the proper characterization of the interface between material phases. It is very common in composite materials that the interface between the matrix and the reinforcement has its own behavior, which is usually weaker than both materials. In that sense, one can treat such an interface (or interphase) as a separate material phase with its own constitutive law. Mean field and homogenization methods accounting for interphase layers between the matrix and the reinforcement have been proposed by several authors [25–30]. In most of these studies, however, the developed frameworks are limited to the elastic response. Recently, a new self-consistent scheme has been proposed [31] for multi-coated particulate- or fiber-reinforced composites experiencing nonlinear behavior. This approach utilizes the transformation field analysis theory of Dvorak and coworkers [32–34] in order to split the overall composite behavior into an elastic and an inelastic part.

In the present work, the scope is to study the local and global behavior of multi-coated particulate- or fiber-reinforced composites with a nonlinear response. To achieve this goal, in the first step the Eshelby's inhomogeneity problem is revisited, considering the presence of a coating layer between the inhomogeneity and the infinite matrix and nonlinear strains in the form of eigenstrains at all phases. The problem is solved using three different approaches: a general methodology for ellipsoidal inhomogeneities and two analytical techniques, focusing on infinitely long cylindrical fibers and spherical particles. Once this step is completed, the extension of the Mori–Tanaka and the self-consistent schemes for composites with coated reinforcement, in the basis of transformation field analysis, allow proper mean field homogenization strategies to be designed.

The organization of the manuscript is as follows. After the introduction, the following four sections discuss procedures for solving Eshelby's inhomogeneity problem of coated fibers or particles embedded in an infinite matrix and undergoing inelastic deformations in the form of fixed eigenstrains in all material phases. The solution of the problem leads to the computation of interaction tensors. Three methodologies are described in these sections: the first is designed for general ellipsoidal shape coated inhomogeneities and is based on the analysis of Berbenni and Cherkaoui [31]. The second considers infinitely long cylindrical fibers with transversely isotropic properties and is developed using appropriate boundary value problems similar to those proposed in the composite cylinder assemblage [35]. The third method refers to spherical isotropic coated particles and utilizes the solution of proper boundary value problems similar to those of the composite sphere assemblage [36]. Section 6 presents two mean field approaches for coated fiber or particle composites, namely the Mori–Tanaka and the self-consistent methods, in which the nonlinear response is accounted for through the transformation field analysis framework [32–34]. The two theories use the defined interaction tensors and provide the overall inelastic response of the composite, as well as the correlation between micro- and macroscopic strain and stress fields. Section 7 presents numerical examples, in which the general methodology [31] is compared with the more accurate composite cylinder assemblage and composite sphere assemblage approaches for coated long cylindrical fibers and spherical particles, respectively. The paper finishes with a conclusions section.

2. Eshelby's coated inhomogeneity problem accounting for eigenstrains

The mean field homogenization theories, for instance, the Mori–Tanaka and self-consistent theories, are formulated using as a key point the Eshelby's well-known inhomogeneity problem: a single ellipsoidal shape inhomogeneity is embedded in an infinite matrix, which is subjected to uniform strain at a far distance. The solution of this basic boundary value problem provides what is known as the interaction tensor or dilute concentration tensor. The latter is a fourth-order tensor that connects the average strain in the inhomogeneity with the applied uniform strain. The various micromechanics approaches utilize this information in a different way to establish appropriate concentration tensors for composite materials with ellipsoidal particles and a matrix phase [7, 37].

Eshelby's inhomogeneity problem has been further extended from its initial version for elastic solids to account for inelastic strains or stresses inside the inhomogeneity [7]. Such an extension allows for the evaluation of inelastic interaction tensors that can be utilized for nonlinear analyses of composite materials, as is the case in the transformation field analysis approach [32, 33]. The aim of this and the following three sections is to provide the solution of Eshelby's inhomogeneity problem, considering coated inhomogeneities with homothetic topology and inelastic strains (called "eigenstrains" in this paper). While the description focuses on single-layer coated inhomogeneities, all the discussed techniques can be applied in a similar fashion for multi-coated inhomogeneities.

Consider a coated ellipsoidal inhomogeneity, embedded in an infinite matrix. The inhomogeneity is characterized by elasticity modulus $\boldsymbol{L}_1$, occupies the space Ω_1 with volume V_1, is bounded by the surface $\partial\Omega_1$ and is subjected to the uniform eigenstrain ε_1^p, which causes eigenstress $\boldsymbol{\sigma}_1^p = -\boldsymbol{L}_1 : \varepsilon_1^p$. The coating layer is characterized by elasticity modulus $\boldsymbol{L}_2$, occupies the space Ω_2 with volume V_2, is bounded by the surfaces $\partial\Omega_1$ and $\partial\Omega_2$ and is subjected to the uniform eigenstrain ε_2^p, which causes eigenstress $\boldsymbol{\sigma}_2^p = -\boldsymbol{L}_2 : \varepsilon_2^p$. The matrix phase is characterized by elasticity modulus $\boldsymbol{L}_0$, occupies the space Ω_0, which extends to infinity, and is subjected to the uniform eigenstrain ε_0^p, which causes eigenstress $\boldsymbol{\sigma}_0^p = -\boldsymbol{L}_0 : \varepsilon_0^p$, while at a far distance a linear displacement field $\boldsymbol{u}_0 = \varepsilon_0 \cdot \boldsymbol{x}$ is applied (Figure 1). The space $\Omega = \Omega_1 \cup \Omega_2 \cup \Omega_0$ denotes the total body, including the matrix and the coated inhomogeneity.

For this problem, the equilibrium equation reads

$$\mathrm{div}\boldsymbol{\sigma} = \boldsymbol{0}, \text{ in } \Omega, \tag{1}$$

with

$$\boldsymbol{\sigma} = \begin{cases} \boldsymbol{L}_0 : \left[\varepsilon - \varepsilon_0^p\right], \boldsymbol{x} \in \Omega_0, \\ \boldsymbol{L}_1 : \left[\varepsilon - \varepsilon_1^p\right], \boldsymbol{x} \in \Omega_1, \\ \boldsymbol{L}_2 : \left[\varepsilon - \varepsilon_2^p\right], \boldsymbol{x} \in \Omega_2. \end{cases} \tag{2}$$

The boundary conditions state that $\varepsilon = \varepsilon_0$ at a far distance from the inhomogeneity.[1]

The goal of this study is to compute the average strains inside the inhomogeneity and inside the coating layer

$$\varepsilon_1 = \frac{1}{V_1}\int_{\Omega_1} \varepsilon(\boldsymbol{x})\mathrm{d}\boldsymbol{x} \text{ and } \varepsilon_2 = \frac{1}{V_2}\int_{\Omega_2} \varepsilon(\boldsymbol{x})\mathrm{d}\boldsymbol{x}, \tag{3}$$

respectively, when the applied strain ε_0 at a far distance and the eigenstrains ε_i^p, $i = 0, 1, 2$, are known. Computing the fourth-order elastic and inelastic interaction tensors $\boldsymbol{T}_1$, $\boldsymbol{T}_2$, $\boldsymbol{T}_{11}^p$, $\boldsymbol{T}_{12}^p$, $\boldsymbol{T}_{10}^p$, $\boldsymbol{T}_{21}^p$, $\boldsymbol{T}_{22}^p$, and $\boldsymbol{T}_{20}^p$, for which

$$\begin{aligned} \varepsilon_1 &= \boldsymbol{T}_1 : \varepsilon_0 + \boldsymbol{T}_{10}^p : \varepsilon_0^p + \boldsymbol{T}_{11}^p : \varepsilon_1^p + \boldsymbol{T}_{12}^p : \varepsilon_2^p, \\ \varepsilon_2 &= \boldsymbol{T}_2 : \varepsilon_0 + \boldsymbol{T}_{20}^p : \varepsilon_0^p + \boldsymbol{T}_{21}^p : \varepsilon_1^p + \boldsymbol{T}_{22}^p : \varepsilon_2^p, \end{aligned} \tag{4}$$

is the goal of the following three sections.

3. Coated ellipsoidal inhomogeneities

For a composite with multi-coated ellipsoidal particles and eigenstresses, Berbenni and Cherkaoui [31] have identified the elastic and inelastic concentration tensors of all phases for the self-consistent method and have obtained the macroscopic response. When considering the Mori–Tanaka method, these global concentration tensors can be translated to dilute concentration tensors, if one substitutes the effective medium with the matrix [37]. This section presents the essential points of the Berbenni and Cherkaoui [31] approach, with proper modifications to meet the needs of this study, for obtaining elastic and inelastic interaction tensors for the coated inhomogeneity.

The spatially varying elastic properties and eigenstresses in the Eshelby problem of Figure 1 can be expressed in the general form

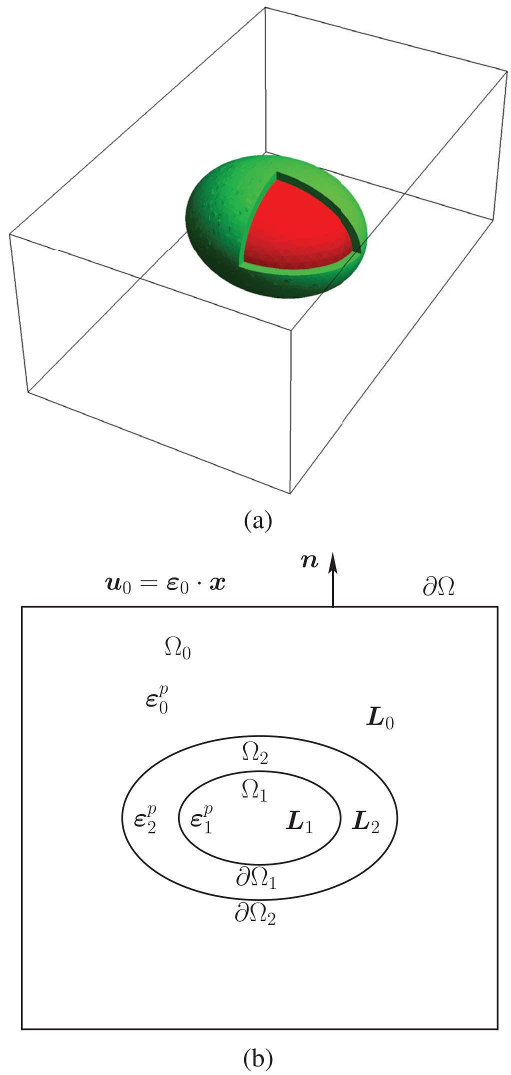

Figure 1. Coated ellipsoidal inhomogeneity with homothetic topology inside a matrix: (a) general view; (b) cross-section. The inhomogeneity, the coating layer, and the matrix have uniform eigenstrains. Moreover, the matrix is subjected to linear displacement at a far distance.

$$\begin{aligned} \boldsymbol{L}(\boldsymbol{x}) &= \boldsymbol{L}_0 + [\boldsymbol{L}_1 - \boldsymbol{L}_0]\theta_1(\boldsymbol{x}) + [\boldsymbol{L}_2 - \boldsymbol{L}_0]\theta_2(\boldsymbol{x}), \\ \boldsymbol{\sigma}^p(\boldsymbol{x}) &= \boldsymbol{\sigma}_0^p + [\boldsymbol{\sigma}_1^p - \boldsymbol{\sigma}_0^p]\theta_1(\boldsymbol{x}) + [\boldsymbol{\sigma}_2^p - \boldsymbol{\sigma}_0^p]\theta_2(\boldsymbol{x}), \end{aligned} \tag{5}$$

for $\forall \boldsymbol{x} \in \Omega = \Omega_1 \cup \Omega_2 \cup \Omega_0$, with

$$\theta_i(\boldsymbol{x}) \begin{cases} 1, & \forall \boldsymbol{x} \in \Omega_i, \\ 0, & \forall \boldsymbol{x} \notin \Omega_i, \end{cases} i = 1, 2. \tag{6}$$

Considering the linear displacement boundary condition $\boldsymbol{u}_0(\boldsymbol{x}) = \varepsilon_0.\boldsymbol{x}$, the Green's formalism defines the strain tensor ε at any point in the space Ω as [33, 31]

$$\varepsilon(\boldsymbol{x}) = \varepsilon_0 - \int_\Omega \boldsymbol{\Gamma}(\boldsymbol{x} - \boldsymbol{x}') : [\boldsymbol{L}(\boldsymbol{x}') - \boldsymbol{L}_0] : \varepsilon(\boldsymbol{x}')\mathrm{d}\boldsymbol{x}' - \int_\Omega \boldsymbol{\Gamma}(\boldsymbol{x} - \boldsymbol{x}') \colon \left[\boldsymbol{\sigma}^p(\boldsymbol{x}') - \boldsymbol{\sigma}_0^p(\boldsymbol{x}')\right]\mathrm{d}\boldsymbol{x}', \tag{7}$$

where $\boldsymbol{\Gamma}(\boldsymbol{x}-\boldsymbol{x}')$ is the modified Green's tensor. The proof of the last expression arises from a straightforward extension of the Korringa methodology [38]. From equations (5) and (6), it becomes clear that the integrands at the right-hand side of equation (7) are nonzero only inside the inhomogeneity and its coating. With this information, equation (7) takes the form

$$\begin{aligned}&\varepsilon(\boldsymbol{x})=\varepsilon_0-\int_{\Omega_c}\boldsymbol{\Gamma}(\boldsymbol{x}-\boldsymbol{x}'):[\boldsymbol{L}(\boldsymbol{x}')-\boldsymbol{L}_0]:\varepsilon(\boldsymbol{x}')\mathrm{d}\boldsymbol{x}'-\int_{\Omega_c}\boldsymbol{\Gamma}(\boldsymbol{x}-\boldsymbol{x}'):\left[\boldsymbol{\sigma}^p(\boldsymbol{x}')-\boldsymbol{\sigma}_0^p(\boldsymbol{x}')\right]\mathrm{d}\boldsymbol{x}',\\&\Omega_c=\Omega_1\cup\Omega_2.\end{aligned}\tag{8}$$

Averaging over the space Ω_c with volume $V_c=V_1+V_2$ yields that the average strain ε_c inside the coated inhomogeneity is given by the expression

$$\begin{aligned}\varepsilon_c&=\frac{1}{V_c}\int_{\Omega_c}\varepsilon(\boldsymbol{x})\mathrm{d}\boldsymbol{x}\\&=\varepsilon_0-\boldsymbol{S}(\boldsymbol{L}_0):\boldsymbol{L}_0^{-1}:\frac{1}{V_c}\int_{\Omega_c}[\boldsymbol{L}(\boldsymbol{x}')-\boldsymbol{L}_0]:\varepsilon(\boldsymbol{x}')\mathrm{d}\boldsymbol{x}'-\boldsymbol{S}(\boldsymbol{L}_0):\boldsymbol{L}_0^{-1}:\frac{1}{V_c}\int_{\Omega_c}\left[\boldsymbol{\sigma}^p(\boldsymbol{x}')-\boldsymbol{\sigma}_0^p(\boldsymbol{x}')\right]\mathrm{d}\boldsymbol{x}',\end{aligned}\tag{9}$$

where $\boldsymbol{S}(\boldsymbol{L}_0)$ is the well- known Eshelby tensor, which depends on the properties $\boldsymbol{L}_0$ of the matrix and the shape of the inhomogeneity [5]. With the help of equations (3), (5), and (6), the last expression is written

$$\begin{aligned}\varepsilon_c=\varepsilon_0&-\frac{V_1}{V_c}\boldsymbol{S}(\boldsymbol{L}_0):\boldsymbol{L}_0^{-1}:[\boldsymbol{L}_1-\boldsymbol{L}_0]:\varepsilon_1-\frac{V_2}{V_c}\boldsymbol{S}(\boldsymbol{L}_0):\boldsymbol{L}_0^{-1}:[\boldsymbol{L}_2-\boldsymbol{L}_0]:\varepsilon_2\\&-\frac{V_1}{V_c}\boldsymbol{S}(\boldsymbol{L}_0):\boldsymbol{L}_0^{-1}:\boldsymbol{\sigma}_1^p-\frac{V_2}{V_c}\boldsymbol{S}(\boldsymbol{L}_0):\boldsymbol{L}_0^{-1}:\boldsymbol{\sigma}_2^p+\boldsymbol{S}(\boldsymbol{L}_0):\boldsymbol{L}_0^{-1}:\boldsymbol{\sigma}_0^p.\end{aligned}\tag{10}$$

Considering that

$$\varepsilon_c=\frac{V_1}{V_c}\varepsilon_1+\frac{V_2}{V_c}\varepsilon_2,\tag{11}$$

equation (10) takes its final form

$$\begin{aligned}&\frac{V_1}{V_c}\left[\mathcal{I}+\boldsymbol{S}(\boldsymbol{L}_0):\boldsymbol{L}_0^{-1}:[\boldsymbol{L}_1-\boldsymbol{L}_0]\right]:\varepsilon+\frac{V_2}{V_c}\left[\mathcal{I}+\boldsymbol{S}(\boldsymbol{L}_0):\boldsymbol{L}_0^{-1}:[\boldsymbol{L}_2-\boldsymbol{L}_0]\right]:\varepsilon_2\\&\quad=\varepsilon_0-\frac{V_1}{V_c}\boldsymbol{S}(\boldsymbol{L}_0):\boldsymbol{L}_0^{-1}:\boldsymbol{\sigma}_1^p-\frac{V_2}{V_c}\boldsymbol{S}(\boldsymbol{L}_0):\boldsymbol{L}_0^{-1}:\boldsymbol{\sigma}_2^p+\boldsymbol{S}(\boldsymbol{L}_0):\boldsymbol{L}_0^{-1}:\boldsymbol{\sigma}_0^p,\end{aligned}\tag{12}$$

where $\mathcal{I}_{ijkl}=[\delta_{ik}\delta_{jl}+\delta_{il}\delta_{jk}]/2$ is the symmetric fourth-order identity tensor and δ_{ij} is the Kronecker delta. The connection between the average strain tensors in the inhomogeneity and the coating is provided with the help of the interfacial operators [39, 40]. The jump of $\boldsymbol{\varepsilon}$ across an interface between two materials is given by [31]

$$\varepsilon^+(\boldsymbol{x})=[\mathcal{I}+\boldsymbol{H}(\boldsymbol{x}):[\boldsymbol{L}_1-\boldsymbol{L}_2]]:\varepsilon^-(\boldsymbol{x})+\boldsymbol{H}(\boldsymbol{x}):\left[\boldsymbol{\sigma}_1^p-\boldsymbol{\sigma}_2^p\right],\tag{13}$$

where $\mathcal{I}$ is the extended identity tensor and $\boldsymbol{H}(\boldsymbol{x})$ is the interfacial operator, which depends on $\boldsymbol{L}_2$ and the unit vector of the inrrterface between the inhomogeneity and the coating layer. At this point, the main approximation is that the strain $\varepsilon^-(\boldsymbol{x})$ is substituted for the average strain ε_1 of the inhomogeneity. With this assumption, accounting for the homothetic topology of the inhomogeneity and the coating layer and averaging equation (13) over the space Ω_2 yields [41]

$$\varepsilon_2=\left[\mathcal{I}+\boldsymbol{S}(\boldsymbol{L}_2):\boldsymbol{L}_2^{-1}:[\boldsymbol{L}_1-\boldsymbol{L}_2]\right]:\varepsilon_1+\boldsymbol{S}(\boldsymbol{L}_2):\boldsymbol{L}_2^{-1}:\boldsymbol{\sigma}_1^p-\boldsymbol{S}(\boldsymbol{L}_2):\boldsymbol{L}_2^{-1}:\boldsymbol{\sigma}_2^p.\tag{14}$$

$\boldsymbol{S}(\boldsymbol{L}_2)$ denotes the Eshelby tensor that depends on the coating layer elasticity tensor and the shape of the inhomogeneity. For a number of coating layers, equations similar to the last one connect the average strains between two adjacent layers. Equation (14) is exact only when the strain inside the inhomogeneity is uniform. Combining equations (12) and (14) and comparing them with equation (4) yields

$$
\begin{aligned}
&\boldsymbol{T}_1 = [\phi \boldsymbol{n}_{10} + [1-\phi]\boldsymbol{n}_{20} : \boldsymbol{n}_{12}]^{-1},\\
&\boldsymbol{T}_2 = \boldsymbol{n}_{12} : \boldsymbol{T}_1,\\
&\boldsymbol{T}^p_{10} = -\ \boldsymbol{T}_1 : \boldsymbol{P}_0 : \boldsymbol{L}_0,\\
&\boldsymbol{T}^p_{11} = \boldsymbol{T}_1 : [\phi \boldsymbol{P}_0 + [1-\phi]\boldsymbol{n}_{20} : \boldsymbol{P}_2] : \boldsymbol{L}_1,\\
&\boldsymbol{T}^p_{12} = [1-\phi]\,\boldsymbol{T}_1 : [\boldsymbol{P}_0 - \boldsymbol{n}_{20} : \boldsymbol{P}_2] : \boldsymbol{L}_2,\\
&\boldsymbol{T}^p_{20} = \boldsymbol{n}_{12} : \boldsymbol{T}^p_{10},\\
&\boldsymbol{T}^p_{21} = \boldsymbol{n}_{12} : \boldsymbol{T}^p_{11} - \boldsymbol{P}_2 : \boldsymbol{L}_1,\\
&\boldsymbol{T}^p_{22} = \boldsymbol{n}_{12} : \boldsymbol{T}^p_{12} + \boldsymbol{P}_2 : \boldsymbol{L}_2,
\end{aligned}
\tag{15}
$$

with

$$
\begin{aligned}
&\boldsymbol{n}_{10} = \mathcal{I} + \boldsymbol{P}_0 : [\boldsymbol{L}_1 - \boldsymbol{L}_0],\\
&\boldsymbol{n}_{20} = \mathcal{I} + \boldsymbol{P}_0 : [\boldsymbol{L}_2 - \boldsymbol{L}_0],\\
&\boldsymbol{n}_{12} = \mathcal{I} + \boldsymbol{P}_2 : [\boldsymbol{L}_1 - \boldsymbol{L}_2],\\
&\boldsymbol{P}_0 = \boldsymbol{S}(\boldsymbol{L}_0) : \boldsymbol{L}_0^{-1},\\
&\boldsymbol{P}_2 = \boldsymbol{S}(\boldsymbol{L}_2) : \boldsymbol{L}_2^{-1},\\
&\phi = \frac{V_1}{V_1 + V_2}.
\end{aligned}
\tag{16}
$$

4. Coated infinitely long cylindrical inhomogeneities

The method discussed in the previous section accounts for general ellipsoidal inhomogeneities and anisotropic behavior of the material constituents. Nevertheless, the drawback is that its accuracy depends on the validity of equation (14). In multi-coated inhomogeneities, the use of interfacial operators between adjacent layers may lead to the accumulation of significant error. In this section, an alternative approach is presented for the case of transversely isotropic material phases and coated infinitely long cylindrical inhomogeneities. This formalism is based on the well-known composite cylinder assemblage [35] and provides the exact solution for the interaction tensors.

Inside the representative volume element, the various mechanical fields generated at every phase q ($q = 0, 1, 2$) depend on the spatial position, i.e.,

$$\boldsymbol{u}^{(q)}(\boldsymbol{x}), \varepsilon^{(q)}(\boldsymbol{x}), \boldsymbol{\sigma}^{(q)}(\boldsymbol{x}), \forall \boldsymbol{x} \in \Omega_q.$$

Owing to the geometry of the inhomogeneities, the problem of Figure 1 can be transformed into cylindrical coordinates, using a system of concentric cylinders for the inhomogeneity, the coating layer, and the infinite matrix (Figure 2). In cylindrical coordinates, the axes (x, y, z) are transformed to (r, θ, z) and the strain tensor components at each phase are given by the expressions

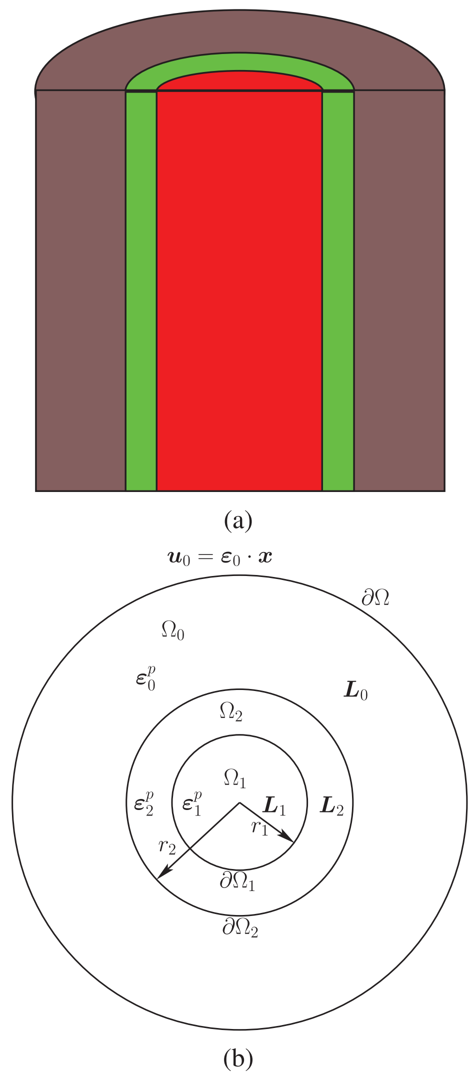

Figure 2. Coated infinitely long cylindrical inhomogeneity with homothetic topology inside a matrix. Cross-section (a) parallel to inhomogeneity and (b) normal to inhomogeneity. All phases have uniform eigenstrains. Moreover, the infinite matrix is subjected to linear displacement at a far distance.

$$
\begin{aligned}
\varepsilon_{rr}^{(q)} &= \frac{\partial u_r^{(q)}}{\partial r}, \\
\varepsilon_{\theta\theta}^{(q)} &= \frac{1}{r}\frac{\partial u_\theta^{(q)}}{\partial \theta} + \frac{u_r^{(q)}}{r}, \\
\varepsilon_{zz}^{(q)} &= \frac{\partial u_z^{(q)}}{\partial z}, \\
2\varepsilon_{r\theta}^{(q)} &= \frac{\partial u_\theta^{(q)}}{\partial r} + \frac{1}{r}\frac{\partial u_r^{(q)}}{\partial \theta} - \frac{u_\theta^{(q)}}{r}, \\
2\varepsilon_{rz}^{(q)} &= \frac{\partial u_z^{(q)}}{\partial r} + \frac{\partial u_r^{(q)}}{\partial z}, \\
2\varepsilon_{\theta z}^{(q)} &= \frac{1}{r}\frac{\partial u_z^{(q)}}{\partial \theta} + \frac{\partial u_\theta^{(q)}}{\partial z},
\end{aligned}
$$

while the equilibrium equations are written as

$$\begin{aligned}
&\frac{\partial \sigma_{rr}^{(q)}}{\partial r}+\frac{1}{r}\frac{\partial \sigma_{r\theta}^{(q)}}{\partial \theta}+\frac{\sigma_{rr}^{(q)}-\sigma_{\theta\theta}^{(q)}}{r}+\frac{\partial \sigma_{rz}^{(q)}}{\partial z}=0,\\
&\frac{\partial \sigma_{r\theta}^{(q)}}{\partial r}+\frac{1}{r}\frac{\partial \sigma_{\theta\theta}^{(q)}}{\partial \theta}+\frac{2\sigma_{r\theta}^{(q)}}{r}+\frac{\partial \sigma_{\theta z}^{(q)}}{\partial z}=0,\\
&\frac{\partial \sigma_{rz}^{(q)}}{\partial r}+\frac{1}{r}\frac{\partial \sigma_{\theta z}^{(q)}}{\partial \theta}+\frac{\sigma_{rz}^{(q)}}{r}+\frac{\partial \sigma_{zz}^{(q)}}{\partial z}=0.
\end{aligned} \tag{17}$$

For transversely isotropic matrix, inhomogeneity, and coating layer, the constitutive law

$$\boldsymbol{\sigma}=\boldsymbol{C}:[\varepsilon-\varepsilon^{p}]$$

is characterized by an elasticity modulus $\mathbf{C}$, written in Voigt notation[2] as

$$\boldsymbol{C}=\begin{bmatrix}
K_q^{\mathrm{tr}}+\mu_q^{\mathrm{tr}} & K_q^{\mathrm{tr}}-\mu_q^{\mathrm{tr}} & l_q & 0 & 0 & 0\\
K_q^{\mathrm{tr}}-\mu_q^{\mathrm{tr}} & K_q^{\mathrm{tr}}+\mu_q^{\mathrm{tr}} & l_q & 0 & 0 & 0\\
l_q & l_q & n_q & 0 & 0 & 0\\
0 & 0 & 0 & \mu_q^{\mathrm{tr}} & 0 & 0\\
0 & 0 & 0 & 0 & \mu_q^{\mathrm{ax}} & 0\\
0 & 0 & 0 & 0 & 0 & \mu_q^{\mathrm{ax}}
\end{bmatrix}.$$

The five constants K_q^{tr}, l_q, n_q, μ_q^{tr}, and μ_q^{ax} are material parameters.

The inhomogeneity is considered to have radius $r=r_1$ and the coating layer has external radius r_2 (Figure 2). The ratio $\phi=r_1^2/r_2^2$ corresponds to the volume fraction $V_1/[V_1+V_2]$. The traction and displacement continuity between the inhomogeneity and the coating layer are expressed through the relations

$$\begin{aligned}
u_r^{(1)}(r_1,\theta,z)&=u_r^{(2)}(r_1,\theta,z),\\
u_\theta^{(1)}(r_1,\theta,z)&=u_\theta^{(2)}(r_1,\theta,z),\\
u_z^{(1)}(r_1,\theta,z)&=u_z^{(2)}(r_1,\theta,z),\\
\sigma_{rr}^{(1)}(r_1,\theta,z)&=\sigma_{rr}^{(2)}(r_1,\theta,z),\\
\sigma_{r\theta}^{(1)}(r_1,\theta,z)&=\sigma_{r\theta}^{(2)}(r_1,\theta,z),\\
\sigma_{rz}^{(1)}(r_1,\theta,z)&=\sigma_{rz}^{(2)}(r_1,\theta,z).
\end{aligned} \tag{18}$$

Additionally, the interface conditions between the coating layer and the matrix are written as

$$\begin{aligned}
u_r^{(2)}(r_2,\theta,z)&=u_r^{(0)}(r_2,\theta,z),\\
u_\theta^{(2)}(r_2,\theta,z)&=u_\theta^{(0)}(r_2,\theta,z),\\
u_z^{(2)}(r_2,\theta,z)&=u_z^{(0)}(r_2,\theta,z),\\
\sigma_{rr}^{(2)}(r_2,\theta,z)&=\sigma_{rr}^{(0)}(r_2,\theta,z),\\
\sigma_{r\theta}^{(2)}(r_2,\theta,z)&=\sigma_{r\theta}^{(0)}(r_2,\theta,z),\\
\sigma_{rz}^{(2)}(r_2,\theta,z)&=\sigma_{rz}^{(0)}(r_2,\theta,z).
\end{aligned} \tag{19}$$

As already discussed, the interaction tensors provide the average strains in the inhomogeneity and the coating layer when the eigenstrains and the boundary strain tensor are known. Using equation (3) and the divergence theorem, the average strain in the inhomogeneity is expressed as

$$\begin{aligned}
\varepsilon_1&=\frac{1}{V_1}\int_{\Omega_1}\varepsilon^{(1)}\,\mathrm{d}V\\
&=\frac{1}{V_1}\int_{\partial\Omega_1}\frac{1}{2}\left[\boldsymbol{u}^{(1)}\otimes\boldsymbol{n}+\boldsymbol{n}\otimes\boldsymbol{u}^{(1)}\right]\mathrm{d}S.
\end{aligned} \tag{20}$$

In this expression, the unit vector $\boldsymbol{n}$ is the same for every interface and the external boundary surface, owing to the homothetic topology. Equation (3), the divergence theorem, and the displacement continuity conditions (equation (19)) define the average strain in the coating layer as

$$\begin{aligned}\varepsilon_2 &= \frac{1}{V_2}\int_{\Omega_2} \varepsilon^{(2)}\,\mathrm{d}V \\ &= \frac{\phi/V_1}{1-\phi}\int_{\partial\Omega_2} \frac{1}{2}\left[\boldsymbol{u}^{(0)}\otimes\boldsymbol{n}+\boldsymbol{n}\otimes\boldsymbol{u}^{(0)}\right]\mathrm{d}S - \frac{\phi}{1-\phi}\varepsilon_1.\end{aligned} \tag{21}$$

In this section, the interaction tensors are computed with the help of analytical solutions for the boundary value problems described by Hashin [42]. In the pure elastic problem, similar techniques have been utilized in the literature to obtain dilute [25] and semi-dilute [43] stress concentration tensors, as well as dilute strain concentration tensors [30] for coated fiber composites.

In cylindrical coordinates, the surface element in a surface of constant radius r (a vertical cylinder) is $\mathrm{d}s_r = r\mathrm{d}\theta\mathrm{d}z$ and the surface element in a surface of constant z is $\mathrm{d}s_z = r\mathrm{d}r\mathrm{d}\theta$. For an arbitrary tensor $\boldsymbol{Q}(r,\theta,z)$ and a cylinder of radius r_q and length $2L$, the sum of surface integrals with the general form

$$\mathcal{F} = \frac{1}{2L\pi r_q}\int_{-L}^{L}\int_0^{2\pi}\boldsymbol{Q}(r_q,\theta,z)\mathrm{d}\theta\mathrm{d}z + \frac{1}{2L\pi r_q^2}\int_0^{2\pi}\int_0^{r_q}[\boldsymbol{Q}(r,\theta,L)-\boldsymbol{Q}(r,\theta,-L)]r\mathrm{d}r\mathrm{d}\theta \tag{22}$$

is required for the computations of the average quantities in equations (20) and (21).[3] The three normal vectors are expressed in cylindrical coordinates as

$$\boldsymbol{n}_1 = \begin{bmatrix}\cos\theta\\ \sin\theta\\ 0\end{bmatrix}, \qquad \boldsymbol{n}_2 = \begin{bmatrix}-\sin\theta\\ \cos\theta\\ 0\end{bmatrix}, \qquad \boldsymbol{n}_3 = \begin{bmatrix}0\\ 0\\ 1\end{bmatrix}. \tag{23}$$

The displacements of the phases are represented in matrix form as

$$\boldsymbol{u}^{(q)} = u_r^{(q)}\boldsymbol{n}_1 + u_\theta^{(q)}\boldsymbol{n}_2 + u_z^{(q)}\boldsymbol{n}_3, \qquad q = 0,1,2. \tag{24}$$

As a final remark before proceeding to the boundary value problems, it is noted that in infinitely long inhomogeneities with isotropic or transversely isotropic phases, the elastic and inelastic interaction tensors present transverse isotropy. In Voigt notation, they take the general forms

$$\begin{aligned}\boldsymbol{T} &= \begin{bmatrix} T_{11} & T_{12} & T_{13} & 0 & 0 & 0\\ T_{12} & T_{11} & T_{13} & 0 & 0 & 0\\ 0 & 0 & 1 & 0 & 0 & 0\\ 0 & 0 & 0 & T_{44} & 0 & 0\\ 0 & 0 & 0 & 0 & T_{55} & 0\\ 0 & 0 & 0 & 0 & 0 & T_{55}\end{bmatrix}, \\ \boldsymbol{T}^p &= \begin{bmatrix} T^p_{11} & T^p_{12} & T^p_{13} & 0 & 0 & 0\\ T^p_{12} & T^p_{11} & T^p_{13} & 0 & 0 & 0\\ 0 & 0 & 0 & 0 & 0 & 0\\ 0 & 0 & 0 & T^p_{44} & 0 & 0\\ 0 & 0 & 0 & 0 & T^p_{55} & 0\\ 0 & 0 & 0 & 0 & 0 & T^p_{55}\end{bmatrix},\end{aligned} \tag{25}$$

with $T_{12} = T_{11} - T_{44}$ and $T^p_{12} = T^p_{11} - T^p_{44}$.

4.1. Axial shear strain conditions

For this case, the following displacement vector is applied at the boundary $\partial\Omega$

$$\boldsymbol{u}_0 = \begin{bmatrix} 0 \\ 0 \\ \beta x \end{bmatrix},$$

which corresponds to the strain tensor (in classical tensorial form)

$$\varepsilon_0 = \frac{\beta}{2} \begin{bmatrix} 0 & 0 & 1 \\ 0 & 0 & 0 \\ 1 & 0 & 0 \end{bmatrix}.$$

In addition, the eigenstrains (in classical tensorial form)

$$\varepsilon_q^p = \frac{s_q}{2} \begin{bmatrix} 0 & 0 & 1 \\ 0 & 0 & 0 \\ 1 & 0 & 0 \end{bmatrix} \qquad \forall \boldsymbol{x} \in \Omega_q,$$

are imposed at every phase. In cylindrical coordinates, the vector $\boldsymbol{u}_0$ and the second-order tensors ε_q^p, $q=0,1,2$, are transformed to the forms

$$\boldsymbol{u}_0^{(r,\theta,z)} = \begin{bmatrix} 0 \\ 0 \\ \beta r \cos\theta \end{bmatrix},$$
$$\varepsilon_q^{p(r,\theta,z)} = \tfrac{s_q}{2} \begin{bmatrix} 0 & 0 & \cos\theta \\ 0 & 0 & -\sin\theta \\ \cos\theta & -\sin\theta & 0 \end{bmatrix}.$$

For these conditions, the displacement vectors at the matrix ($q=0$), the inhomogeneity ($q=1$), and the coating layer ($q=2$) are given by the general expressions

$$u_z^{(q)}(r,\theta) = \beta r U_z^{(q)}(r) \cos\theta, \qquad u_r^{(q)} = u_\theta^{(q)} = 0,$$
$$U_z^{(q)}(r) = \Xi_1^{(q)} + \Xi_2^{(q)} \frac{1}{[r/r_1]^2},$$

where $\Xi_i^{(q)}$, $i=1,2$, are unknown constants. These general expressions lead to stresses that satisfy the equilibrium equations (17). The important stresses for identifying the unknown constants are

$$\sigma_{rz}^{(q)}(r,\theta) = \left[\beta \Sigma_{rz}^{(q)}(r) - \mu_q^{\mathrm{ax}} s_q\right] \cos\theta,$$
$$\Sigma_{rz}^{(q)}(r) = \mu_q^{\mathrm{ax}} \left[\Xi_1^{(q)} - \Xi_2^{(q)} \frac{1}{[r/r_1]^2}\right].$$

The boundary conditions that should be satisfied in this boundary value problem are

$$u_z^{(1)} \text{ finite at } r=0 \rightarrow \Xi_2^{(1)} = 0,$$
$$u_z^{(0)}(r \rightarrow \infty, \theta) = \beta r \cos\theta \rightarrow \Xi_1^{(0)} = 1.$$

Considering these results, the interface conditions (equations (18) and (19)) construct the linear system

$$\boldsymbol{K} \,.\, \Xi = \boldsymbol{F} + \frac{s_0}{\beta}\boldsymbol{F}_0 + \frac{s_1}{\beta}\boldsymbol{F}_1 + \frac{s_2}{\beta}\boldsymbol{F}_2,$$

with

$$
\boldsymbol{K} = \begin{bmatrix} 1 & -1 & -1 & 0 \\ \mu_1^{\mathrm{ax}} & -\mu_2^{\mathrm{ax}} & \mu_2^{\mathrm{ax}} & 0 \\ 0 & 1 & \phi & -\phi \\ 0 & \mu_2^{\mathrm{ax}} & -\phi\mu_2^{\mathrm{ax}} & \phi\mu_0^{\mathrm{ax}} \end{bmatrix},
$$

$$
\boldsymbol{\Xi} = \begin{bmatrix} \Xi_1^{(1)} & \Xi_1^{(2)} & \Xi_2^{(2)} & \Xi_2^{(0)} \end{bmatrix}^{\mathrm{T}},
$$

$$
\boldsymbol{F} = \begin{bmatrix} 0 & 0 & 1 & \mu_0^{\mathrm{ax}} \end{bmatrix}^{\mathrm{T}},
$$

$$
\boldsymbol{F}_0 = \begin{bmatrix} 0 & 0 & 0 & -\mu_0^{\mathrm{ax}} \end{bmatrix}^{\mathrm{T}},
$$

$$
\boldsymbol{F}_1 = \begin{bmatrix} 0 & \mu_1^{\mathrm{ax}} & 0 & 0 \end{bmatrix}^{\mathrm{T}},
$$

$$
\boldsymbol{F}_2 = \begin{bmatrix} 0 & -\mu_2^{\mathrm{ax}} & 0 & \mu_2^{\mathrm{ax}} \end{bmatrix}^{\mathrm{T}}.
$$

The solution of this linear system gives the terms $\Xi_1^{(1)}$ and $\Xi_2^{(0)}$ in the forms

$$
\Xi_1^{(1)} = B_1 + \frac{s_0}{\beta} B_2 + \frac{s_1}{\beta} B_3 + \frac{s_2}{\beta} B_4,
$$

$$
\Xi_2^{(0)} = B_5 + \frac{s_0}{\beta} B_6 + \frac{s_1}{\beta} B_7 + \frac{s_2}{\beta} B_8.
$$

Implementing equations (22), (23), and (24) in equations (20) and (21) yields the average strain inside the inhomogeneity and the coating layer,

$$
\varepsilon_1 = \frac{\beta}{2} U_z^{(1)}(r_1) \begin{bmatrix} 0 & 0 & 1 \\ 0 & 0 & 0 \\ 1 & 0 & 0 \end{bmatrix},
$$

$$
\varepsilon_2 = \frac{1}{1-\phi} U_z^{(0)}(r_2) \frac{\beta}{2} \begin{bmatrix} 0 & 0 & 1 \\ 0 & 0 & 0 \\ 1 & 0 & 0 \end{bmatrix} - \frac{\phi}{1-\phi} \varepsilon_1.
$$

Comparing these results with equation (25), it becomes clear that

$$
\begin{aligned}
T_{1_{55}} &= \frac{\varepsilon_{1_{xz}}}{\beta/2} \Big|_{s_0 = s_1 = s_2 = 0} = B_1, \\
T^p_{10_{55}} &= \frac{\varepsilon_{1_{xz}}}{s_0/2} \Big|_{\beta = s_1 = s_2 = 0} = B_2, \\
T^p_{11_{55}} &= \frac{\varepsilon_{1_{xz}}}{s_1/2} \Big|_{\beta = s_0 = s_2 = 0} = B_3, \\
T^p_{12_{55}} &= \frac{\varepsilon_{1_{xz}}}{s_2/2} \Big|_{\beta = s_0 = s_1 = 0} = B_4, \\
T_{2_{55}} &= \frac{\varepsilon_{2_{xz}}}{\beta/2} \Big|_{s_0 = s_1 = s_2 = 0} = \frac{1 + \phi[B_5 - B_1]}{1-\phi}, \\
T^p_{20_{55}} &= \frac{\varepsilon_{2_{xz}}}{s_0/2} \Big|_{\beta = s_1 = s_2 = 0} = \frac{\phi[B_6 - B_2]}{1-\phi}, \\
T^p_{21_{55}} &= \frac{\varepsilon_{2_{xz}}}{s_1/2} \Big|_{\beta = s_0 = s_2 = 0} = \frac{\phi[B_7 - B_3]}{1-\phi}, \\
T^p_{22_{55}} &= \frac{\varepsilon_{2_{xz}}}{s_2/2} \Big|_{\beta = s_0 = s_1 = 0} = \frac{\phi[B_8 - B_4]}{1-\phi}.
\end{aligned}
\tag{26}
$$

4.2. Transverse shear strain conditions

For this case, the following displacement vector is applied at the boundary $\partial\Omega$

$$\boldsymbol{u}_0 = \begin{bmatrix} \beta y \\ \beta x \\ 0 \end{bmatrix},$$

which corresponds to the strain tensor (in classical tensorial form)

$$\varepsilon_0 = \beta \begin{bmatrix} 0 & 1 & 0 \\ 1 & 0 & 0 \\ 0 & 0 & 0 \end{bmatrix}.$$

In addition, the eigenstrains (in classical tensorial form)

$$\varepsilon_q^p = s_q \begin{bmatrix} 0 & 1 & 0 \\ 1 & 0 & 0 \\ 0 & 0 & 0 \end{bmatrix} \qquad \forall \boldsymbol{x} \in \Omega_q,$$

are imposed at every phase. In cylindrical coordinates, the vector $\boldsymbol{u}_0$ and the second-order tensors $\boldsymbol{\varepsilon}_q^p$, $q = 0, 1, 2$, are transformed to the forms

$$\boldsymbol{u}_0^{(r,\theta,z)} = \begin{bmatrix} \beta r \sin 2\theta \\ \beta r \cos 2\theta \\ 0 \end{bmatrix},$$

$$\varepsilon_q^{p(r,\theta,z)} = s_q \begin{bmatrix} \sin 2\theta & \cos 2\theta & 0 \\ \cos 2\theta & -\sin 2\theta & 0 \\ 0 & 0 & 0 \end{bmatrix}.$$

For these conditions, the displacement vectors at the matrix ($q = 0$), the inhomogeneity ($q = 1$), and the coating layer ($q = 2$) are given by the general expressions

$$\begin{aligned}
& u_r^{(q)}(r,\theta) = \beta r U_r^{(q)}(r) \sin 2\theta, \\
& U_r^{(q)}(r) = \frac{K_q^{\mathrm{tr}} - \mu_q^{\mathrm{tr}}}{2K_q^{\mathrm{tr}} + \mu_q^{\mathrm{tr}}} [r/r_1]^2 \Xi_1^{(q)} + \Xi_2^{(q)} \\
& - \frac{1}{[r/r_1]^4} \Xi_3^{(q)} + \frac{K_q^{\mathrm{tr}} + \mu_q^{\mathrm{tr}}}{\mu_q^{\mathrm{tr}}} \frac{1}{[r/r_1]^2} \Xi_4^{(q)}, \\
& u_\theta^{(q)}(r,\theta) = \beta r U_\theta^{(q)}(r) \cos 2\theta, \\
& U_\theta^{(q)}(r) = [r/r_1]^2 \Xi_1^{(q)} + \Xi_2^{(q)} + \frac{1}{[r/r_1]^4} \Xi_3^{(q)} + \frac{1}{[r/r_1]^2} \Xi_4^{(q)},
\end{aligned}$$

where $\Xi_i^{(q)}$, $i = 1, 2, 3, 4$, are unknown constants. Moreover, $u_z = 0$ everywhere. These general expressions lead to stresses that satisfy the equilibrium equations (equation (17)). The important stresses for identifying the unknown constants are

$$\sigma_{rr}^{(q)}(r,\theta) = \left[\beta \Sigma_{rr}^{(q)}(r) - 2\mu_q^{\mathrm{tr}} s_q\right] \sin 2\theta\,,$$

$$\Sigma_{rr}^{(q)}(r) = 2\mu_q^{\mathrm{tr}} \Xi_2^{(q)} + 6\mu_q^{\mathrm{tr}} \frac{1}{[r/r_1]^4} \Xi_3^{(q)} - 4K_q^{\mathrm{tr}} \frac{1}{[r/r_1]^2} \Xi_4^{(q)}\,,$$

$$\sigma_{r\theta}^{(q)}(r,\theta) = \left[\beta \Sigma_{r\theta}^{(q)}(r) - 2\mu_q^{\mathrm{tr}} s_q\right] \cos 2\theta\,,$$

$$\Sigma_{r\theta}^{(q)}(r) = \frac{6K_q^{\mathrm{tr}}\mu_q^{\mathrm{tr}}}{2K_q^{\mathrm{tr}} + \mu_q^{\mathrm{tr}}} [r/r_1]^2 \Xi_1^{(q)} + 2\mu_q^{\mathrm{tr}} \Xi_2^{(q)}$$

$$-6\mu_q^{\mathrm{tr}} \tfrac{1}{[r/r_1]^4} \Xi_3^{(q)} + 2K_q^{\mathrm{tr}} \tfrac{1}{[r/r_1]^2} \Xi_4^{(q)}\,.$$

The boundary conditions that should be satisfied in this boundary value problem are

$$u_r^{(1)}, u_\theta^{(1)} \text{ finite at } r=0 \rightarrow \Xi_3^{(1)} = \Xi_4^{(1)} = 0\,,$$

$$\left.\begin{array}{l} u_r^{(0)}(r\rightarrow\infty,\theta) = \beta r \sin 2\theta \\ u_\theta^{(0)}(r\rightarrow\infty,\theta) = \beta r \cos 2\theta \end{array}\right\} \rightarrow \Xi_1^{(0)} = 0, \Xi_2^{(0)} = 1\,.$$

Considering these results, the interface conditions (equation (18) and (19)) construct the linear system

$$\boldsymbol{K}\,.\,\boldsymbol{\Xi} = \boldsymbol{F} + \frac{s_0}{\beta}\boldsymbol{F}_0 + \frac{s_1}{\beta}\boldsymbol{F}_1 + \frac{s_2}{\beta}\boldsymbol{F}_2,$$

with

$$\boldsymbol{K} = \begin{bmatrix} K_{11} & 1 & K_{13} & -1 & 1 & K_{16} & 0 & 0 \\ 1 & 1 & -1 & -1 & -1 & -1 & 0 & 0 \\ 0 & K_{32} & 0 & K_{34} & K_{35} & K_{36} & 0 & 0 \\ K_{41} & K_{42} & K_{43} & K_{44} & K_{45} & K_{46} & 0 & 0 \\ 0 & 0 & K_{53} & 1 & -\phi^2 & K_{56} & \phi^2 & K_{58} \\ 0 & 0 & 1/\phi & 1 & \phi^2 & \phi & -\phi^2 & \phi \\ 0 & 0 & 0 & K_{74} & K_{75} & K_{76} & K_{77} & K_{78} \\ 0 & 0 & K_{83} & K_{84} & K_{85} & K_{86} & K_{87} & K_{88} \end{bmatrix},$$

$$\boldsymbol{\Xi} = \left[\Xi_1^{(1)}\ \ \Xi_2^{(1)}\ \ \Xi_1^{(2)}\ \ \Xi_2^{(2)}\ \ \Xi_3^{(2)}\ \ \Xi_4^{(2)}\ \ \Xi_3^{(0)}\ \ \Xi_4^{(0)}\right]^{\mathrm{T}},$$

$$\boldsymbol{F} = \left[0\ \ 0\ \ 0\ \ 0\ \ 1\ \ 1\ \ 2\mu_0^{\mathrm{tr}}\ \ 2\mu_0^{\mathrm{tr}}\right]^{\mathrm{T}},$$

$$\boldsymbol{F}_0 = \left[0\ \ 0\ \ 0\ \ 0\ \ 0\ \ 0 - 2\mu_0^{\mathrm{tr}}\ \ - 2\mu_0^{\mathrm{tr}}\right]^{\mathrm{T}},$$

$$\boldsymbol{F}_1 = \left[0\ \ 0\ \ 2\mu_1^{\mathrm{tr}}\ \ 2\mu_1^{\mathrm{tr}}\ \ 0\ \ 0\ \ 0\ \ 0\right]^{\mathrm{T}},$$

$$\boldsymbol{F}_2 = \left[0\ \ 0\ \ - 2\mu_2^{\mathrm{tr}}\ \ - 2\mu_2^{\mathrm{tr}}\ \ 0\ \ 0\ \ 2\mu_2^{\mathrm{tr}}\ \ 2\mu_2^{\mathrm{tr}}\right]^{\mathrm{T}},$$

and

$$\begin{gathered}
K_{11}=\frac{K_1^{\mathrm{tr}}-\mu_1^{\mathrm{tr}}}{2K_1^{\mathrm{tr}}+\mu_1^{\mathrm{tr}}}, \qquad -K_{13}=\phi K_{53}=\frac{K_2^{\mathrm{tr}}-\mu_2^{\mathrm{tr}}}{2K_2^{\mathrm{tr}}+\mu_2^{\mathrm{tr}}},\\
K_{41}=\frac{6K_1^{\mathrm{tr}}\mu_1^{\mathrm{tr}}}{2K_1^{\mathrm{tr}}+\mu_1^{\mathrm{tr}}}, \qquad -K_{16}=\frac{K_{56}}{\phi}=\frac{K_2^{\mathrm{tr}}+\mu_2^{\mathrm{tr}}}{\mu_2^{\mathrm{tr}}},\\
-K_{58}=\phi\frac{K_0^{\mathrm{tr}}+\mu_0^{\mathrm{tr}}}{\mu_0^{\mathrm{tr}}}, \qquad -K_{43}=\phi K_{83}=\frac{6K_2^{\mathrm{tr}}\mu_2^{\mathrm{tr}}}{2K_2^{\mathrm{tr}}+\mu_2^{\mathrm{tr}}},\\
-K_{34}=-K_{44}=K_{74}=K_{84}=2\mu_2^{\mathrm{tr}},\\
-K_{35}=K_{45}=K_{75}/\phi^2=-K_{85}/\phi^2=6\mu_2^{\mathrm{tr}},\\
2K_{36}=-K_{46}=-2K_{76}/\phi=K_{86}/\phi=2K_2^{\mathrm{tr}},\\
K_{32}=K_{42}=2\mu_1^{\mathrm{tr}}, \qquad -K_{77}=K_{87}=6\phi^2\mu_0^{\mathrm{tr}},\\
2K_{78}=-K_{88}=2\phi K_0^{\mathrm{tr}}.
\end{gathered}$$

The solution of this linear system gives the terms $\Xi_1^{(1)}$, $\Xi_2^{(1)}$, and $\Xi_4^{(0)}$ in the forms

$$\begin{aligned}
\Xi_1^{(1)}&=B_1+\frac{s_0}{\beta}B_2+\frac{s_1}{\beta}B_3+\frac{s_2}{\beta}B_4,\\
\Xi_2^{(1)}&=B_5+\frac{s_0}{\beta}B_6+\frac{s_1}{\beta}B_7+\frac{s_2}{\beta}B_8,\\
\Xi_4^{(0)}&=B_9+\frac{s_0}{\beta}B_{10}+\frac{s_1}{\beta}B_{11}+\frac{s_2}{\beta}B_{12}.
\end{aligned}$$

Implementing equations (22), (23), and (24) in equations (20) and (21) yields the average strain inside the inhomogeneity and the coating layer,

$$\begin{aligned}
\varepsilon_1&=\frac{\beta}{2}\left[U_r^{(1)}(r_1)+U_\theta^{(1)}(r_1)\right]\begin{bmatrix}0&1&0\\1&0&0\\0&0&0\end{bmatrix},\\
\varepsilon_2&=\frac{1}{1-\phi}\frac{\beta}{2}\left[U_r^{(0)}(r_2)+U_\theta^{(0)}(r_2)\right]\begin{bmatrix}0&1&0\\1&0&0\\0&0&0\end{bmatrix}-\frac{\phi}{1-\phi}\varepsilon_1.
\end{aligned}$$

Comparing these results with equation (25), it becomes clear that

$$\begin{aligned}
T_{1_{44}}&=\frac{\varepsilon_{1_{xy}}}{\beta}\Big|_{s_0=s_1=s_2=0}=\frac{3K_1^{\mathrm{tr}}}{4K_1^{\mathrm{tr}}+2\mu_1^{\mathrm{tr}}}B_1+B_5,\\
T^p_{10_{44}}&=\frac{\varepsilon_{1_{xy}}}{s_0}\Big|_{\beta=s_1=s_2=0}=\frac{3K_1^{\mathrm{tr}}}{4K_1^{\mathrm{tr}}+2\mu_1^{\mathrm{tr}}}B_2+B_6,\\
T^p_{11_{44}}&=\frac{\varepsilon_{1_{xy}}}{s_1}\Big|_{\beta=s_0=s_2=0}=\frac{3K_1^{\mathrm{tr}}}{4K_1^{\mathrm{tr}}+2\mu_1^{\mathrm{tr}}}B_3+B_7,\\
T^p_{12_{44}}&=\frac{\varepsilon_{1_{xy}}}{s_2}\Big|_{\beta=s_0=s_1=0}=\frac{3K_1^{\mathrm{tr}}}{4K_1^{\mathrm{tr}}+2\mu_1^{\mathrm{tr}}}B_4+B_8,\\
T_{2_{44}}&=\frac{\varepsilon_{2_{xy}}}{\beta}\Big|_{s_0=s_1=s_2=0}=-\frac{\phi}{1-\phi}T_{1_{44}}+\frac{1}{1-\phi}\left[1+\phi\frac{K_0^{\mathrm{tr}}+2\mu_0^{\mathrm{tr}}}{2\mu_0^{\mathrm{tr}}}B_9\right],\\
T^p_{20_{44}}&=\frac{\varepsilon_{2_{xy}}}{s_0}\Big|_{\beta=s_1=s_2=0}=\frac{\phi}{1-\phi}\frac{K_0^{\mathrm{tr}}+2\mu_0^{\mathrm{tr}}}{2\mu_0^{\mathrm{tr}}}B_{10}-\frac{\phi}{1-\phi}T^p_{10_{44}},\\
T^p_{21_{44}}&=\frac{\varepsilon_{2_{xy}}}{s_1}\Big|_{\beta=s_0=s_2=0}=\frac{\phi}{1-\phi}\frac{K_0^{\mathrm{tr}}+2\mu_0^{\mathrm{tr}}}{2\mu_0^{\mathrm{tr}}}B_{11}-\frac{\phi}{1-\phi}T^p_{11_{44}},\\
T^p_{22_{44}}&=\frac{\varepsilon_{2_{xy}}}{s_2}\Big|_{\beta=s_0=s_1=0}=\frac{\phi}{1-\phi}\frac{K_0^{\mathrm{tr}}+2\mu_0^{\mathrm{tr}}}{2\mu_0^{\mathrm{tr}}}B_{12}-\frac{\phi}{1-\phi}T^p_{12_{44}}.
\end{aligned}\tag{27}$$

4.3. Plane strain conditions

For this case, the following displacement vector is applied at the boundary $\partial\Omega$

$$\boldsymbol{u}_0 = \begin{bmatrix} \beta x \\ \beta y \\ 0 \end{bmatrix},$$

which corresponds to the strain tensor (in classical tensorial form)

$$\varepsilon_0 = \beta \begin{bmatrix} 1 & 0 & 0 \\ 0 & 1 & 0 \\ 0 & 0 & 0 \end{bmatrix}.$$

In addition, the eigenstrains (in classical tensorial form)

$$\boldsymbol{\varepsilon}_q^p = s_q \begin{bmatrix} 1 & 0 & 0 \\ 0 & 1 & 0 \\ 0 & 0 & 0 \end{bmatrix} \quad \forall\, \boldsymbol{x} \in \boldsymbol{\Omega}_q,$$

are imposed at every phase. In cylindrical coordinates, the vector $\boldsymbol{u}_0$ is expressed as

$$\boldsymbol{u}_0^{(r,\theta,z)} = \begin{bmatrix} \beta r \\ 0 \\ 0 \end{bmatrix},$$

while the second-order tensors ε_q^p, $q = 0, 1, 2$, retain their form. For these conditions, the displacement vectors at the matrix ($q = 0$), the inhomogeneity ($q = 1$), and the coating layer ($q = 2$) are given by the general expressions

$$u_r^{(q)}(r,\theta) = \beta r U_r^{(q)}(r), \qquad u_\theta^{(q)} = u_z^{(q)} = 0,$$
$$U_r^{(q)}(r) = \Xi_1^{(q)} + \Xi_2^{(q)} \frac{1}{[r/r_1]^2},$$

where $\Xi_i^{(q)}$, $i = 1, 2$, are unknown constants. These general expressions lead to stresses that satisfy the equilibrium equations (equation (17)). The important stresses for identifying the unknown constants are

$$\sigma_{rr}^{(q)}(r) = \beta \Sigma_{rr}^{(q)}(r) - 2K_q^{\mathrm{tr}} s_q,$$
$$\Sigma_{rr}^{(q)}(r) = 2K_q^{\mathrm{tr}} \Xi_1^{(q)} - 2\mu_q^{\mathrm{tr}} \Xi_2^{(q)} \frac{1}{[r/r_1]^2}.$$

The boundary conditions that should be satisfied in this boundary value problem are

$$u_r^{(1)} \text{ finite at } r = 0 \rightarrow \Xi_2^{(1)} = 0,$$
$$u_r^{(0)}(r \rightarrow \infty) = \beta r \rightarrow \Xi_1^{(0)} = 1.$$

Considering these results, the interface conditions (equations (18) and (19)) construct the linear system

$$\boldsymbol{K} \,.\, \boldsymbol{\Xi} = \boldsymbol{F} + \frac{s_0}{\beta}\boldsymbol{F}_0 + \frac{s_1}{\beta}\boldsymbol{F}_1 + \frac{s_2}{\beta}\boldsymbol{F}_2,$$

with

$$\boldsymbol{K}=\begin{bmatrix} 1 & -1 & -1 & 0 \\ 2K_1^{\mathrm{tr}} & -2K_2^{\mathrm{tr}} & 2\mu_2^{\mathrm{tr}} & 0 \\ 0 & 1 & \phi & -\phi \\ 0 & 2K_2^{\mathrm{tr}} & -2\phi\mu_2^{\mathrm{tr}} & 2\phi\mu_0^{\mathrm{tr}} \end{bmatrix},$$
$$\boldsymbol{\Xi}=\begin{bmatrix} \Xi_1^{(1)} & \Xi_1^{(2)} & \Xi_2^{(2)} & \Xi_2^{(0)} \end{bmatrix}^{\mathrm{T}},$$
$$\boldsymbol{F}=\begin{bmatrix} 0 & 0 & 1 & 2K_0^{\mathrm{tr}} \end{bmatrix}^{\mathrm{T}},$$
$$\boldsymbol{F}_0=\begin{bmatrix} 0 & 0 & 0 & -2K_0^{\mathrm{tr}} \end{bmatrix}^{\mathrm{T}},$$
$$\boldsymbol{F}_1=\begin{bmatrix} 0 & 2K_1^{\mathrm{tr}} & 0 & 0 \end{bmatrix}^{\mathrm{T}},$$
$$\boldsymbol{F}_2=\begin{bmatrix} 0 & -2K_2^{\mathrm{tr}} & 0 & 2K_2^{\mathrm{tr}} \end{bmatrix}^{\mathrm{T}}.$$

The solution of this linear system gives the terms $\Xi_1^{(1)}$ and $\Xi_2^{(0)}$ in the forms

$$\Xi_1^{(1)}=B_1+\frac{s_0}{\beta}B_2+\frac{s_1}{\beta}B_3+\frac{s_2}{\beta}B_4,$$
$$\Xi_2^{(0)}=B_5+\frac{s_0}{\beta}B_6+\frac{s_1}{\beta}B_7+\frac{s_2}{\beta}B_8.$$

Implementing equations (22), (23) and (24) in equations (20) and (21) yields the average strain inside the inhomogeneity and the coating layer,

$$\varepsilon_1=\beta U_r^{(1)}(r_1)\begin{bmatrix} 1 & 0 & 0 \\ 0 & 1 & 0 \\ 0 & 0 & 0 \end{bmatrix},$$
$$\varepsilon_2=\frac{\beta}{1-\phi}U_r^{(0)}(r_2)\begin{bmatrix} 1 & 0 & 0 \\ 0 & 1 & 0 \\ 0 & 0 & 1 \end{bmatrix}-\frac{\phi}{1-\phi}\varepsilon_1.$$

Equation (25) enables one to write

$$\varepsilon_{1_{xx}}=[2T_{1_{11}}-T_{1_{44}}]\beta+\left[2T^p_{10_{11}}-T^p_{10_{44}}\right]s_0+\left[2T^p_{11_{11}}-T^p_{11_{44}}\right]s_1+\left[2T^p_{12_{11}}-T^p_{12_{44}}\right]s_2,$$
$$\varepsilon_{2_{xx}}=[2T_{2_{11}}-T_{2_{44}}]\beta+\left[2T^p_{20_{11}}-T^p_{20_{44}}\right]s_0+\left[2T^p_{21_{11}}-T^p_{21_{44}}\right]s_1+\left[2T^p_{22_{11}}-T^p_{22_{44}}\right]s_2.$$

From these relations, it becomes clear that

$$T_{1_{11}}=\frac{1}{2}[B_1+T_{1_{44}}],$$
$$T^p_{10_{11}}=\frac{1}{2}\left[B_2+T^p_{10_{44}}\right],$$
$$T^p_{11_{11}}=\frac{1}{2}\left[B_3+T^p_{11_{44}}\right],$$
$$T^p_{12_{11}}=\frac{1}{2}\left[B_4+T^p_{12_{44}}\right],$$
$$T_{2_{11}}=\frac{1+\phi[B_5-B_1]}{2[1-\phi]}+\frac{T_{2_{44}}}{2},$$
$$T^p_{20_{11}}=\frac{\phi[B_6-B_2]}{2[1-\phi]}+\frac{T^p_{20_{44}}}{2},$$

$$
\begin{aligned}
T^p_{21_{11}} &= \frac{\phi[B_7 - B_3]}{2[1-\phi]} + \frac{T^p_{21_{44}}}{2}, \\
T^p_{22_{11}} &= \frac{\phi[B_8 - B_4]}{2[1-\phi]} + \frac{T^p_{22_{44}}}{2}.
\end{aligned} \tag{28}
$$

4.4. Hydrostatic strain conditions

For this case, the following displacement vector is applied at the boundary $\partial\Omega$

$$
\boldsymbol{u}_0 = \begin{bmatrix} \beta x \\ \beta y \\ \beta z \end{bmatrix},
$$

which corresponds to the strain tensor (in classical tensorial form)

$$
\varepsilon_0 = \beta \begin{bmatrix} 1 & 0 & 0 \\ 0 & 1 & 0 \\ 0 & 0 & 1 \end{bmatrix}.
$$

In addition, the eigenstrains (in classical tensorial form)

$$
\varepsilon^p_q = s_q \begin{bmatrix} 1 & 0 & 0 \\ 0 & 1 & 0 \\ 0 & 0 & 1 \end{bmatrix} \quad \forall\ \boldsymbol{x} \in \boldsymbol{\Omega}_q,
$$

are imposed at every phase. In cylindrical coordinates, the vector $\boldsymbol{u}_0$

$$
\boldsymbol{u}_0^{(r,\theta,z)} = \begin{bmatrix} \beta r \\ 0 \\ \beta z \end{bmatrix},
$$

while the second-order tensors ε^p_q, $q = 0, 1, 2$, retain their form. For these conditions, the displacement vectors at the matrix ($q = 0$), the inhomogeneity ($q = 1$), and the coating layer ($q = 2$) are given by the general expressions

$$
\begin{aligned}
&u_r^{(q)}(r) = \beta r U_r^{(q)}(r), \qquad u_\theta^{(q)} = 0, \qquad u_z^{(q)}(z) = \beta z, \\
&U_r^{(q)}(r) = \Xi_1^{(q)} + \Xi_2^{(q)} \frac{1}{[r/r_1]^2},
\end{aligned}
$$

where $\Xi_i^{(q)}$, $i = 1, 2$, are unknown constants. These general expressions lead to stresses that satisfy the equilibrium equations (equation (17)). The important stresses for identifying the unknown constants are

$$
\begin{aligned}
&\sigma_{rr}^{(q)}(r) = \beta \Sigma_{rr}^{(q)}(r) - [2K_q^{\mathrm{tr}} + l_q] s_q, \\
&\Sigma_{rr}^{(q)}(r) = 2K_q^{\mathrm{tr}} \Xi_1^{(q)} - 2\mu_q^{\mathrm{tr}} \Xi_2^{(q)} \frac{1}{[r/r_1]^2} + l_q.
\end{aligned}
$$

The boundary conditions that should be satisfied in this boundary value problem are

$$
\begin{aligned}
u_r^{(1)} \ \text{finite at}\ r = 0 &\rightarrow \Xi_2^{(1)} = 0, \\
u_r^{(0)}(r \rightarrow \infty) = \beta r &\rightarrow \Xi_1^{(0)} = 1.
\end{aligned}
$$

Considering these results, the interface conditions (equation (18) and (19)) construct the linear system

$$\boldsymbol{K}\,.\,\boldsymbol{\Xi}=\boldsymbol{F}+\frac{s_0}{\beta}\boldsymbol{F}_0+\frac{s_1}{\beta}\boldsymbol{F}_1+\frac{s_2}{\beta}\boldsymbol{F}_2,$$

with

$$\boldsymbol{K}=\begin{bmatrix} 1 & -1 & -1 & 0 \\ 2K_1^{\mathrm{tr}} & -2K_2^{\mathrm{tr}} & 2\mu_2^{\mathrm{tr}} & 0 \\ 0 & 1 & \phi & -\phi \\ 0 & 2K_2^{\mathrm{tr}} & -2\phi\mu_2^{\mathrm{tr}} & 2\phi\mu_0^{\mathrm{tr}} \end{bmatrix},$$
$$\boldsymbol{\Xi}=\begin{bmatrix} \Xi_1^{(1)} & \Xi_1^{(2)} & \Xi_2^{(2)} & \Xi_2^{(0)} \end{bmatrix}^{\mathrm{T}},$$
$$\boldsymbol{F}=\begin{bmatrix} 0 & l_2-l_1 & 1 & 2K_0^{\mathrm{tr}}+l_0-l_2 \end{bmatrix}^{\mathrm{T}},$$
$$\boldsymbol{F}_0=\begin{bmatrix} 0 & 0 & 0 & -2K_0^{\mathrm{tr}}-l_0 \end{bmatrix}^{\mathrm{T}},$$
$$\boldsymbol{F}_1=\begin{bmatrix} 0 & 2K_1^{\mathrm{tr}}+l_1 & 0 & 0 \end{bmatrix}^{\mathrm{T}},$$
$$\boldsymbol{F}_2=\begin{bmatrix} 0 & -2K_2^{\mathrm{tr}}-l_2 & 0 & 2K_2^{\mathrm{tr}}+l_2 \end{bmatrix}^{\mathrm{T}}.$$

The solution of this linear system gives the terms $\Xi_1^{(1)}$ and $\Xi_2^{(0)}$ in the forms

$$\Xi_1^{(1)}=B_1+\frac{s_0}{\beta}B_2+\frac{s_1}{\beta}B_3+\frac{s_2}{\beta}B_4,$$
$$\Xi_2^{(0)}=B_5+\frac{s_0}{\beta}B_6+\frac{s_1}{\beta}B_7+\frac{s_2}{\beta}B_8.$$

Implementing equations (22), (23) and (24) in equations (20) and (21) yields the average strain inside the inhomogeneity and the coating layer,

$$\varepsilon_1=\beta U_r^{(1)}(r_1)\begin{bmatrix} 1 & 0 & 0 \\ 0 & 1 & 0 \\ 0 & 0 & 1 \end{bmatrix},$$
$$\varepsilon_2=\tfrac{\beta}{1-\phi}U_r^{(0)}(r_2)\begin{bmatrix} 1 & 0 & 0 \\ 0 & 1 & 0 \\ 0 & 0 & 1 \end{bmatrix}-\tfrac{\phi}{1-\phi}\varepsilon_1.$$

Equation (25) enables one to write

$$\begin{aligned}\varepsilon_{1_{xx}}&=[2T_{1_{11}}-T_{1_{44}}+T_{1_{13}}]\beta+\left[2T^p_{10_{11}}-T^p_{10_{44}}+T^p_{10_{13}}\right]s_0\\&+\left[2T^p_{11_{11}}-T^p_{11_{44}}+T^p_{11_{13}}\right]s_1+\left[2T^p_{12_{11}}-T^p_{12_{44}}+T^p_{12_{13}}\right]s_2,\\ \varepsilon_{2_{xx}}&=[2T_{2_{11}}-T_{2_{44}}+T_{2_{13}}]\beta+\left[2T^p_{20_{11}}-T^p_{20_{44}}+T^p_{20_{13}}\right]s_0\\&+\left[2T^p_{21_{11}}-T^p_{21_{44}}+T^p_{21_{13}}\right]s_1+\left[2T^p_{22_{11}}-T^p_{22_{44}}+T^p_{22_{13}}\right]s_2.\end{aligned}$$

From these relations, it becomes clear that

$$
\begin{aligned}
T_{1_{13}} &= B_1 - 2T_{1_{11}} + T_{1_{44}},\\
T^p_{10_{13}} &= B_2 - 2T^p_{10_{11}} + T^p_{10_{44}},\\
T^p_{11_{13}} &= B_3 - 2T^p_{11_{11}} + T^p_{11_{44}},\\
T^p_{12_{13}} &= B_4 - 2T^p_{12_{11}} + T^p_{12_{44}},\\
T_{2_{13}} &= \frac{1+\phi[B_5 - B_1]}{1-\phi} - 2T_{2_{11}} + T_{2_{44}},\\
T^p_{20_{13}} &= \frac{\phi[B_6 - B_2]}{1-\phi} - 2T^p_{20_{11}} + T^p_{20_{44}},\\
T^p_{21_{13}} &= \frac{\phi[B_7 - B_3]}{1-\phi} - 2T^p_{21_{11}} + T^p_{21_{44}},\\
T^p_{22_{13}} &= \frac{\phi[B_8 - B_4]}{1-\phi} - 2T^p_{22_{11}} + T^p_{22_{44}}.
\end{aligned} \tag{29}
$$

To conclude, the four discussed boundary value problems provide equations (26), (27), (28), and (29), which enable computation of the elastic and inelastic interaction tensors, which in turn are utilized in micromechanics schemes, such as the Mori–Tanaka and self-consistent schemes.

5. Coated spherical inhomogeneities

Apart from the case of infinitely long cylindrical fibers with transversely isotropic properties, analytical expressions for the interaction tensors can also be obtained for isotropic spherical particles embedded in an isotropic matrix. These expressions are derived through the well-known composite sphere assemblage [44].

The spherical form of the inhomogeneities enables the problem of Figure 1 to be transformed to a system of concentric spheres for the inhomogeneity, the coating layer, and the infinite matrix (Figure 3). In such a structure, it is preferred to utilize the spherical coordinate system. In spherical coordinates, the axes (x, y, z) are transformed to (r, θ, φ) and the strain tensor components at each phase are given by the expressions

$$
\begin{aligned}
\varepsilon^{(q)}_{rr} &= \frac{\partial u^{(q)}_r}{\partial r},\\
\varepsilon^{(q)}_{\theta\theta} &= \frac{1}{r}\frac{\partial u^{(q)}_\theta}{\partial \theta} + \frac{u^{(q)}_r}{r},\\
\varepsilon^{(q)}_{\varphi\varphi} &= \frac{1}{r\sin\theta}\frac{\partial u^{(q)}_\varphi}{\partial \varphi} + \frac{u^{(q)}_r}{r} + \frac{u^{(q)}_\theta \cos\theta}{r\sin\theta},\\
2\varepsilon^{(q)}_{r\theta} &= \frac{\partial u^{(q)}_\theta}{\partial r} + \frac{1}{r}\frac{\partial u^{(q)}_r}{\partial \theta} - \frac{u^{(q)}_\theta}{r},\\
2\varepsilon^{(q)}_{r\varphi} &= \frac{\partial u^{(q)}_\varphi}{\partial r} + \frac{1}{r\sin\theta}\frac{\partial u^{(q)}_r}{\partial \varphi} - \frac{u^{(q)}_\varphi}{r},\\
2\varepsilon^{(q)}_{\theta\varphi} &= \frac{1}{r}\frac{\partial u^{(q)}_\varphi}{\partial \theta} + \frac{1}{r\sin\theta}\frac{\partial u^{(q)}_\theta}{\partial \varphi} - \frac{u^{(q)}_\varphi \cos\theta}{r\sin\theta},
\end{aligned}
$$

while the equilibrium equations are written as

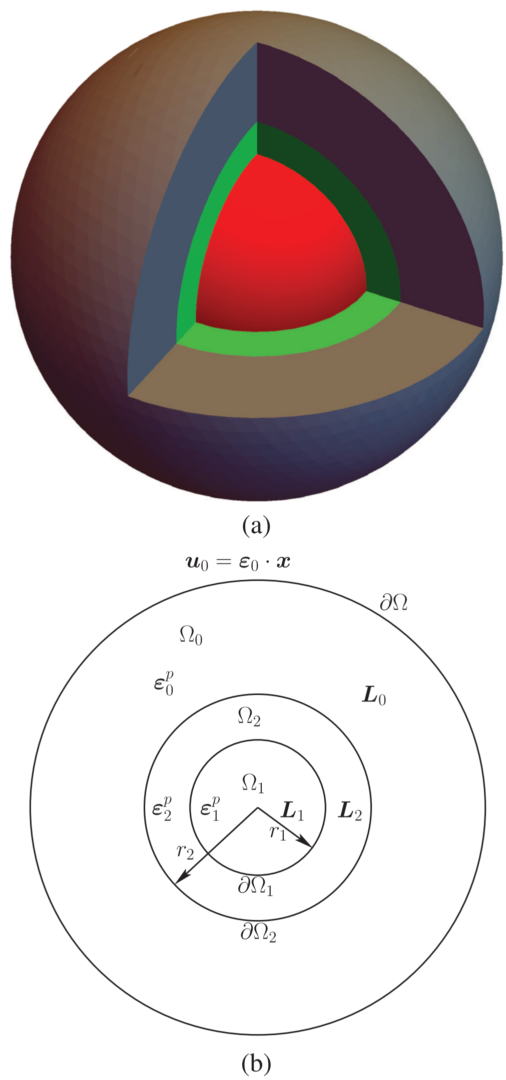

Figure 3. Coated spherical inhomogeneity with homothetic topology inside a matrix: (a) general view and (b) cross-section. The inhomogeneity, the coating layer, and the matrix have uniform eigenstrains. Moreover, the matrix is subjected to linear displacement at a far distance.

$$
\begin{aligned}
&\frac{\partial \sigma_{rr}^{(q)}}{\partial r} + \frac{1}{r}\frac{\partial \sigma_{r\theta}^{(q)}}{\partial \theta} + \frac{\sigma_{r\theta}^{(q)} \cos\theta}{r \sin\theta} + \frac{2\sigma_{rr}^{(q)} - \sigma_{\theta\theta}^{(q)} - \sigma_{\varphi\varphi}^{(q)}}{r} + \frac{1}{r\sin\theta}\frac{\partial \sigma_{r\varphi}^{(q)}}{\partial \varphi} = 0,\\
&\frac{\partial \sigma_{r\theta}^{(q)}}{\partial r} + \frac{1}{r}\frac{\partial \sigma_{\theta\theta}^{(q)}}{\partial \theta} + \frac{3\sigma_{r\theta}^{(q)}}{r} + \frac{\left[\sigma_{\theta\theta}^{(q)} - \sigma_{\varphi\varphi}^{(q)}\right]\cos\theta}{r\sin\theta} + \frac{1}{r\sin\theta}\frac{\partial \sigma_{\theta\varphi}^{(q)}}{\partial \varphi} = 0,\\
&\frac{\partial \sigma_{r\varphi}^{(q)}}{\partial r} + \frac{1}{r}\frac{\partial \sigma_{\theta\varphi}^{(q)}}{\partial \theta} + \frac{3\sigma_{r\varphi}^{(q)}}{r} + \frac{2\sigma_{\theta\varphi}^{(q)}\cos\theta}{r\sin\theta} + \frac{1}{r\sin\theta}\frac{\partial \sigma_{\varphi\varphi}^{(q)}}{\partial \varphi} = 0.
\end{aligned}
\tag{30}
$$

For isotropic phases, the stress is connected with the total and the inelastic strain through the relation

$$\boldsymbol{\sigma} = \boldsymbol{C} : [\varepsilon - \varepsilon^p],$$

Where[4]

$$\boldsymbol{C}=\begin{bmatrix} K_q+\frac{4}{3}\mu_q & K_q-\frac{2}{3}\mu_q & K_q-\frac{2}{3}\mu_q & 0 & 0 & 0 \\ K_q-\frac{2}{3}\mu_q & K_q+\frac{4}{3}\mu_q & K_q-\frac{2}{3}\mu_q & 0 & 0 & 0 \\ K_q-\frac{2}{3}\mu_q & K_q-\frac{2}{3}\mu_q & K_q+\frac{4}{3}\mu_q & 0 & 0 & 0 \\ 0 & 0 & 0 & \mu_q & 0 & 0 \\ 0 & 0 & 0 & 0 & \mu_q & 0 \\ 0 & 0 & 0 & 0 & 0 & \mu_q \end{bmatrix}.$$

The inhomogeneity is considered to have radius $r=r_1$ and the coating layer has external radius r_2 (Figure 3). The ratio $\phi=r_1^3/r_2^3$ corresponds to the volume fraction $V_1/[V_1+V_2]$. The interface conditions between the inhomogeneity and the coating layer are expressed as

$$\begin{aligned} u_r^{(1)}(r_1,\theta,\varphi)&=u_r^{(2)}(r_1,\theta,\varphi),\\ u_\theta^{(1)}(r_1,\theta,\varphi)&=u_\theta^{(2)}(r_1,\theta,\varphi),\\ u_\varphi^{(1)}(r_1,\theta,\varphi)&=u_\varphi^{(2)}(r_1,\theta,\varphi),\\ \sigma_{rr}^{(1)}(r_1,\theta,\varphi)&=\sigma_{rr}^{(2)}(r_1,\theta,\varphi),\\ \sigma_{r\theta}^{(1)}(r_1,\theta,\varphi)&=\sigma_{r\theta}^{(2)}(r_1,\theta,\varphi),\\ \sigma_{r\varphi}^{(1)}(r_1,\theta,\varphi)&=\sigma_{r\varphi}^{(2)}(r_1,\theta,\varphi). \end{aligned} \tag{31}$$

Additionally, the interface conditions between the coating layer and the matrix are written as

$$\begin{aligned} u_r^{(2)}(r_2,\theta,\varphi)&=u_r^{(0)}(r_2,\theta,\varphi),\\ u_\theta^{(2)}(r_2,\theta,\varphi)&=u_\theta^{(0)}(r_2,\theta,\varphi),\\ u_\varphi^{(2)}(r_2,\theta,\varphi)&=u_\varphi^{(0)}(r_2,\theta,\varphi),\\ \sigma_{rr}^{(2)}(r_2,\theta,\varphi)&=\sigma_{rr}^{(0)}(r_2,\theta,\varphi),\\ \sigma_{r\theta}^{(2)}(r_2,\theta,\varphi)&=\sigma_{r\theta}^{(0)}(r_2,\theta,\varphi),\\ \sigma_{r\varphi}^{(2)}(r_2,\theta,\varphi)&=\sigma_{r\varphi}^{(0)}(r_2,\theta,\varphi). \end{aligned} \tag{32}$$

In this section, the interaction tensors are computed analytically with the help of analytical solutions for the boundary value problems described by Hashin [36]. In the pure elastic problem, similar techniques have been reported in the literature to obtain elastic interaction tensors for coated particulate composites [29].

In spherical coordinates, the surface element in a surface of constant radius r is $\mathrm{d}s_r=r^2\cos\theta\mathrm{d}\theta\mathrm{d}\varphi$. For an arbitrary tensor $\boldsymbol{Q}(r,\theta,\varphi)$ and a sphere of radius r_q, the surface integral with the general form

$$\mathcal{F}=\frac{3}{4\pi r_1}\int_0^{2\pi}\int_0^{\pi}\boldsymbol{Q}(r_1,\theta,\varphi)\sin\theta\mathrm{d}\theta\mathrm{d}\varphi \tag{33}$$

is required for the computations of the average quantities (equations (20) and (21)). The three normal vectors in spherical coordinates are expressed as

$$\boldsymbol{n}_1=\begin{bmatrix}\sin\theta\cos\varphi\\ \sin\theta\sin\varphi\\ \cos\theta\end{bmatrix},\qquad \boldsymbol{n}_2=\begin{bmatrix}\cos\theta\cos\varphi\\ \cos\theta\sin\varphi\\ -\sin\theta\end{bmatrix},\qquad \boldsymbol{n}_3=\begin{bmatrix}-\sin\varphi\\ \cos\varphi\\ 0\end{bmatrix}. \tag{34}$$

The displacements of the phases are represented in matrix form as

$$\boldsymbol{u}^{(q)}=u_r^{(q)}\boldsymbol{n}_1+u_\theta^{(q)}\boldsymbol{n}_2+u_\varphi^{(q)}\boldsymbol{n}_3,\qquad q=0,1,2. \tag{35}$$

As a final remark before proceeding to the boundary value problems, it is noted that in spherical inhomogeneities with isotropic phases, the elastic and inelastic interaction tensors present isotropy. In Hill notation, they take the general forms

$$\begin{aligned} \boldsymbol{T} &= 3T_b\boldsymbol{\mathcal{I}}^h + 2T_s\boldsymbol{\mathcal{I}}^d, & \boldsymbol{T}^p &= 3T_b^p\boldsymbol{\mathcal{I}}^h + 2T_s^p\boldsymbol{\mathcal{I}}^d, \\ \boldsymbol{\mathcal{I}}^h &= \frac{1}{3}\boldsymbol{I}\otimes\boldsymbol{I}, & \boldsymbol{\mathcal{I}}^d &= \boldsymbol{\mathcal{I}} - \boldsymbol{\mathcal{I}}^h, \end{aligned} \tag{36}$$

where $I_{ij} = \delta_{ij}$ is the second-order identity tensor. The same formalism is utilized for every fourth-order isotropic tensor.

5.1. Hydrostatic strain conditions

For this case, the following displacement vector is applied at the boundary $\partial\Omega$

$$\boldsymbol{u}_0 = \begin{bmatrix} \beta x \\ \beta y \\ \beta z \end{bmatrix},$$

which corresponds to the strain tensor (in classical tensorial form)

$$\varepsilon_0 = \beta \begin{bmatrix} 1 & 0 & 0 \\ 0 & 1 & 0 \\ 0 & 0 & 1 \end{bmatrix}.$$

In addition, the eigenstrains (in classical tensorial form)

$$\varepsilon_q^p = s_q \begin{bmatrix} 1 & 0 & 0 \\ 0 & 1 & 0 \\ 0 & 0 & 1 \end{bmatrix} \qquad \forall \boldsymbol{x} \in \Omega_q,$$

are imposed at all phases. In spherical coordinates, the vector $\boldsymbol{u}_0$

$$\boldsymbol{u}_0^{(r,\theta,\varphi)} = \begin{bmatrix} \beta r \\ 0 \\ 0 \end{bmatrix},$$

while the second-order tensors ε_q^p, $q = 0, 1, 2$, retain their form. For these conditions, the displacement vectors at the matrix ($q = 0$), the inhomogeneity ($q = 1$), and the coating layer ($q = 2$) are given by the general expressions

$$\begin{aligned} u_r^{(q)}(r) &= \beta r U_r^{(q)}(r), \qquad u_\theta^{(q)} = u_\varphi^{(q)} = 0, \\ U_r^{(q)}(r) &= \Xi_1^{(q)} + \Xi_2^{(q)} \frac{1}{[r/r_1]^3}, \end{aligned}$$

where $\Xi_i^{(q)}$, $i = 1, 2$, are unknown constants. These general expressions lead to stresses that satisfy the equilibrium equations (equation (30)). The important stresses for identifying the unknown constants are

$$\begin{aligned} \sigma_{rr}^{(q)}(r) &= \beta\Sigma_{rr}^{(q)}(r) - 3K_q s_q, \\ \Sigma_{rr}^{(q)}(r) &= 3K_q\Xi_1^{(q)} - 4\mu_q\Xi_2^{(q)} \frac{1}{[r/r_1]^3}. \end{aligned}$$

The boundary conditions that should be satisfied in this boundary value problem are

$$u_r^{(1)} \text{ finite at } r=0 \rightarrow \Xi_2^{(1)}=0,$$
$$u_r^{(0)}(r\rightarrow\infty)=\beta r \rightarrow \Xi_1^{(0)}=1\,.$$

Considering these results, the interface conditions (equation (31) and (32)) construct the linear system

$$\boldsymbol{K}\,.\,\boldsymbol{\Xi}=\boldsymbol{F}+\frac{s_0}{\beta}\boldsymbol{F}_0+\frac{s_1}{\beta}\boldsymbol{F}_1+\frac{s_2}{\beta}\boldsymbol{F}_2,$$

with

$$\boldsymbol{K}=\begin{bmatrix} 1 & -1 & -1 & 0 \\ 3K_1 & -3K_2 & 4\mu_2 & 0 \\ 0 & 1 & \phi & -\phi \\ 0 & 3K_2 & -4\phi\mu_2 & 4\phi\mu_0 \end{bmatrix},$$
$$\boldsymbol{\Xi}=\begin{bmatrix}\Xi_1^{(1)} & \Xi_1^{(2)} & \Xi_2^{(2)} & \Xi_2^{(0)}\end{bmatrix},$$
$$\boldsymbol{F}=[0 \quad 0 \quad 1 \quad 3K_0],$$
$$\boldsymbol{F}_0=[0 \quad 0 \quad 0 \quad -3K_0],$$
$$\boldsymbol{F}_1=[0 \quad 3K_1 \quad 0 \quad 0],$$
$$\boldsymbol{F}_2=[0 \quad -3K_2 \quad 0 \quad 3K_2].$$

The solution of this linear system gives the terms $\Xi_1^{(1)}$ and $\Xi_2^{(0)}$ in the forms

$$\Xi_1^{(1)}=B_1+\frac{s_0}{\beta}B_2+\frac{s_1}{\beta}B_3+\frac{s_2}{\beta}B_4,$$
$$\Xi_2^{(0)}=B_5+\frac{s_0}{\beta}B_6+\frac{s_1}{\beta}B_7+\frac{s_2}{\beta}B_8.$$

Implementing equations (33), (34) and (35) in equation (20) and (21) yields the average strain inside the inhomogeneity and the coating layer,

$$\varepsilon_1=\beta U_r^{(1)}(r_1)\begin{bmatrix}1&0&0\\0&1&0\\0&0&1\end{bmatrix},$$
$$\varepsilon_2=\tfrac{\beta}{1-\phi}U_r^{(0)}(r_2)\begin{bmatrix}1&0&0\\0&1&0\\0&0&1\end{bmatrix}-\tfrac{\phi}{1-\phi}\varepsilon_1.$$

Comparing these results with equation (36), it becomes clear that

$$3T_{1_b}=\frac{\mathrm{tr}(\varepsilon_1)}{3\beta}\Big|_{s_0=s_1=s_2=0}=B_1,$$
$$3T^p_{10_b}=\frac{\mathrm{tr}(\varepsilon_1)}{3s_0}\Big|_{\beta=s_1=s_2=0}=B_2,$$
$$3T^p_{11_b}=\frac{\mathrm{tr}(\varepsilon_1)}{3s_1}\Big|_{\beta=s_0=s_2=0}=B_3,$$
$$3T^p_{12_b}=\frac{\mathrm{tr}(\varepsilon_1)}{3s_2}\Big|_{\beta=s_0=s_1=0}=B_4,$$
$$3T_{2_b}=\frac{\mathrm{tr}(\varepsilon_2)}{3\beta}\Big|_{s_0=s_1=s_2=0}=\frac{1+\phi[B_5-B_1]}{1-\phi},$$

$$
\begin{aligned}
3T^{p}_{20_b} &= \frac{\mathrm{tr}(\varepsilon_2)}{3s_0}\Big|_{\beta=s_1=s_2=0} = \frac{\phi[B_6-B_2]}{1-\phi},\\
3T^{p}_{21_b} &= \frac{\mathrm{tr}(\varepsilon_2)}{3s_1}\Big|_{\beta=s_0=s_2=0} = \frac{\phi[B_7-B_3]}{1-\phi},\\
3T^{p}_{22_b} &= \frac{\mathrm{tr}(\varepsilon_2)}{3s_2}\Big|_{\beta=s_0=s_1=0} = \frac{\phi[B_8-B_4]}{1-\phi}.
\end{aligned}
\tag{37}
$$

5.2. Deviatoric strain conditions

For this case, the following displacement vector is applied at the boundary $\partial\Omega$

$$
\boldsymbol{u}_0 = \begin{bmatrix} -\beta x \\ -\beta y \\ 2\beta z \end{bmatrix},
$$

which corresponds to the strain tensor (in classical tensorial form)

$$
\varepsilon_0 = \beta \begin{bmatrix} -1 & 0 & 0 \\ 0 & -1 & 0 \\ 0 & 0 & 2 \end{bmatrix}.
$$

In addition, the eigenstrains (in classical tensorial form)

$$
\varepsilon^{p}_{q} = s_q \begin{bmatrix} -1 & 0 & 0 \\ 0 & -1 & 0 \\ 0 & 0 & 2 \end{bmatrix} \qquad \forall \boldsymbol{x} \in \Omega_q,
$$

are imposed at all phases. In spherical coordinates, the vector $\boldsymbol{u}_0$ and the second-order tensors ε^{p}_{q}, $q=0,1,2$, are written

$$
\boldsymbol{u}_0^{(r,\theta,\varphi)} = \begin{bmatrix} 2\beta r R(\theta) \\ \beta r \dot{R}(\theta) \\ 0 \end{bmatrix},
$$

$$
\varepsilon^{p(r,\theta,\varphi)}_{q} = s_q \begin{bmatrix} 2R(\theta) & \dot{R}(\theta) & 0 \\ \dot{R}(\theta) & -2R(\theta) & 0 \\ 0 & 0 & -1 \end{bmatrix},
$$

where

$$
R(\theta) = \frac{1}{2}[3\cos^2\theta - 1], \qquad \dot{R}(\theta) = \frac{\mathrm{d}R}{\mathrm{d}\theta} = -\,3\cos\theta\sin\theta.
$$

For these conditions, the displacement vectors at the matrix ($q=0$), the inhomogeneity ($q=1$), and the coating layer ($q=2$) are given by the general expressions

$$
\begin{aligned}
u_r^{(q)}(r,\theta) &= \beta r U_r^{(q)}(r) R(\theta)\,,\\
U_r^{(q)}(r) &= 12\nu_q [r/r_1]^2 \Xi_1^{(q)} + 2\Xi_2^{(q)}\\
&\qquad + \frac{10-8\nu_q}{[r/r_1]^3}\Xi_3^{(q)} - \frac{3}{[r/r_1]^5}\Xi_4^{(q)}\,,\\
u_\theta^{(q)}(r,\theta) &= \beta r U_\theta^{(q)}(r)\dot{R}(\theta)\,,\\
U_\theta^{(q)}(r) &= [7-4\nu_q][r/r_1]^2 \Xi_1^{(q)} + \Xi_2^{(q)}\\
&\qquad + \frac{2-4\nu_q}{[r/r_1]^3}\Xi_3^{(q)} + \frac{1}{[r/r_1]^5}\Xi_4^{(q)}\,,
\end{aligned}
$$

where $\Xi_i^{(q)}$, $i = 1, 2, 3, 4$, are unknown constants and

$$
\nu_q = \frac{3K_q - 2\mu_q}{6K_q + 2\mu_q},
$$

is the Poisson's ratio of the qth phase. These general expressions lead to stresses that satisfy the equilibrium equations (equation (30)). The important stresses for identifying the unknown constants are

$$
\begin{aligned}
\sigma_{rr}^{(i)}(r,\theta) &= \left[\beta \Sigma_{rr}^{(q)}(r) - 4\mu_q s_q\right] R(\theta)\,,\\
\Sigma_{rr}^{(q)}(r) &= 4\mu_q \left[-3\nu_q [r/r_1]^2 \Xi_1^{(q)} + \Xi_2^{(q)} - \frac{10-2\nu_q}{[r/r_1]^3}\Xi_3^{(q)} + \frac{6}{[r/r_1]^5}\Xi_4^{(q)}\right],\\
\sigma_{r\theta}^{(i)}(r,\theta) &= \left[\beta \Sigma_{r\theta}^{(q)}(r) - 2\mu_q s_q\right] \dot{R}(\theta)\,,\\
\Sigma_{r\theta}^{(q)}(r) &= 2\mu_q \left[\left[7+2\nu_q\right][r/r_1]^2 \Xi_1^{(q)} + \Xi_2^{(q)} + \frac{2+2\nu_q}{[r/r_1]^3}\Xi_3^{(q)} - \frac{4}{[r/r_1]^5}\Xi_4^{(q)}\right].
\end{aligned}
$$

The boundary conditions that should be satisfied in this boundary value problem are

$$
u_r^{(1)}, u_\theta^{(1)} \text{ finite at } r = 0 \rightarrow \Xi_3^{(1)} = \Xi_4^{(1)} = 0,
$$

$$
\left.\begin{aligned}
u_r^{(0)}(r\to\infty,\theta) &= 2\beta r R(\theta)\\
u_\theta^{(0)}(r\to\infty,\theta) &= \beta r \dot{R}(\theta)
\end{aligned}\right\} \rightarrow \Xi_1^{(0)} = 0, \Xi_2^{(0)} = 1\,.
$$

Considering these results, the interface conditions (equation (31) and (32)) construct the linear system

$$
\boldsymbol{K}\,.\,\boldsymbol{\Xi} = \boldsymbol{F} + \frac{s_0}{\beta}\boldsymbol{F}_0 + \frac{s_1}{\beta}\boldsymbol{F}_1 + \frac{s_2}{\beta}\boldsymbol{F}_2,
$$

with

$$
\boldsymbol{K} = \begin{bmatrix}
K_{11} & 2 & K_{13} & -2 & K_{15} & 3 & 0 & 0\\
K_{21} & 1 & K_{23} & -1 & K_{25} & -1 & 0 & 0\\
K_{31} & K_{32} & K_{33} & K_{34} & K_{35} & K_{36} & 0 & 0\\
K_{41} & K_{42} & K_{43} & K_{44} & K_{45} & K_{46} & 0 & 0\\
0 & 0 & K_{53} & 2 & K_{55} & K_{56} & K_{57} & K_{58}\\
0 & 0 & K_{63} & 1 & K_{65} & K_{66} & K_{67} & K_{68}\\
0 & 0 & K_{73} & K_{74} & K_{75} & K_{76} & K_{77} & K_{78}\\
0 & 0 & K_{83} & K_{84} & K_{85} & K_{86} & K_{87} & K_{88}
\end{bmatrix},
$$

$$
\begin{aligned}
\boldsymbol{\Xi} &= \left[\Xi_1^{(1)} \quad \Xi_2^{(1)} \quad \Xi_1^{(2)} \quad \Xi_2^{(2)} \quad \Xi_3^{(2)} \quad \Xi_4^{(2)} \quad \Xi_3^{(0)} \quad \Xi_4^{(0)}\right]^{\mathrm{T}},\\
\boldsymbol{F} &= [0 \quad 0 \quad 0 \quad 0 \quad 2 \quad 1 \quad 4\mu_0 \quad 2\mu_0]^{\mathrm{T}},\\
\boldsymbol{F}_0 &= [0 \quad 0 \quad 0 \quad 0 \quad 0 \quad 0 \quad -4\mu_0 \quad -2\mu_0]^{\mathrm{T}},\\
\boldsymbol{F}_1 &= [0 \quad 0 \quad 4\mu_1 \quad 2\mu_1 \quad 0 \quad 0 \quad 0 \quad 0]^{\mathrm{T}},\\
\boldsymbol{F}_2 &= [0 \quad 0 \quad -4\mu_2 \quad -2\mu_2 \quad 0 \quad 0 \quad 4\mu_2 \quad 2\mu_2]^{\mathrm{T}},
\end{aligned}
$$

and

$$
\begin{aligned}
&K_{11} = 12\nu_1, \qquad K_{13} = -\,12\nu_2, \qquad K_{15} = -\,10 + 8\nu_2,\\
&K_{21} = 7 - 4\nu_1, \qquad K_{23} = -\,7 + 4\nu_2, \qquad K_{25} = -\,2 + 4\nu_2,\\
&K_{31} = -\,12\mu_1\nu_1, \qquad K_{32} = 4\mu_1, \qquad K_{33} = 12\mu_2\nu_2,\\
&K_{34} = -\,4\mu_2, \qquad K_{35} = 40\mu_2 - 8\mu_2\nu_2, \qquad K_{36} = -\,24\mu_2,\\
&K_{41} = 14\mu_1 + 4\mu_1\nu_1, \qquad K_{42} = 2\mu_1, \qquad K_{43} = -\,14\mu_2 - 4\mu_2\nu_2,\\
&K_{44} = -\,2\mu_2, K_{45} = -\,4\mu_2 - 4\mu_2\nu_2, \qquad K_{46} = 8\mu_2,\\
&K_{53} = 12\nu_2\phi^{-2/3}, \qquad K_{55} = 10\phi - 8\nu_2\phi,\\
&K_{56} = -\,3\phi^{5/3}, \qquad K_{57} = -\,10\phi + 8\nu_0\phi, \qquad K_{58} = 3\phi^{5/3},\\
&K_{63} = [7 - 4\nu_2]\phi^{-2/3}, \qquad K_{65} = 2\phi - 4\nu_2\phi,\\
&K_{66} = \phi^{5/3}, \qquad K_{67} = -\,2\phi + 4\nu_0\phi, \qquad K_{68} = -\,\phi^{5/3},\\
&K_{73} = -\,12\mu_2\nu_2\phi^{-2/3}, \qquad K_{74} = 4\mu_2, \qquad K_{75} = -\,4\mu_2[10 - 2\nu_2]\phi,\\
&K_{76} = 24\mu_2\phi^{5/3}, \qquad K_{77} = 4\mu_0[10 - 2\nu_0]\phi, \qquad K_{78} = -\,24\mu_0\phi^{5/3},\\
&K_{83} = 2\mu_2[7 + 2\nu_2]\phi^{-2/3}, \qquad K_{84} = 2\mu_2, \qquad K_{85} = 2\mu_2[2 + 2\nu_2]\phi,\\
&K_{86} = -\,8\mu_2\phi^{5/3}, \qquad K_{87} = -\,2\mu_0[2 + 2\nu_0]\phi, \qquad K_{88} = 8\mu_0\phi^{5/3}.
\end{aligned}
$$

The solution of this linear system gives the terms $\Xi_1^{(1)}$, $\Xi_2^{(1)}$, and $\Xi_3^{(0)}$ in the forms

$$
\begin{aligned}
\Xi_1^{(1)} &= B_1 + \frac{s_0}{\beta}B_2 + \frac{s_1}{\beta}B_3 + \frac{s_2}{\beta}B_4,\\
\Xi_2^{(1)} &= B_5 + \frac{s_0}{\beta}B_6 + \frac{s_1}{\beta}B_7 + \frac{s_2}{\beta}B_8,\\
\Xi_3^{(0)} &= B_9 + \frac{s_0}{\beta}B_{10} + \frac{s_1}{\beta}B_{11} + \frac{s_2}{\beta}B_{12}.
\end{aligned}
$$

Implementing equations (33), (34) and (35) in equations (20) and (21) yields the average strain inside the inhomogeneity and the coating layer,

$$
\begin{aligned}
\varepsilon_1 &= \frac{\beta}{5}\left[U_r^{(1)}(r_1) + 3U_\theta^{(1)}(r_1)\right]\begin{bmatrix} -1 & 0 & 0\\ 0 & -1 & 0\\ 0 & 0 & 2\end{bmatrix},\\
\varepsilon_2 &= \frac{\beta/5}{1-\phi}\left[U_r^{(0)}(r_2) + 3U_\theta^{(0)}(r_2)\right]\begin{bmatrix} -1 & 0 & 0\\ 0 & -1 & 0\\ 0 & 0 & 2\end{bmatrix} - \frac{\phi}{1-\phi}\varepsilon_1.
\end{aligned}
$$

Comparing these results with equation (36), it becomes clear that

$$
\begin{aligned}
2T_{1_s} &= \frac{-\varepsilon_{1_{xx}}}{\beta}|_{s_0=s_1=s_2=0} = \frac{21}{5}B_1 + B_5,\\
2T^p_{10_s} &= \frac{-\varepsilon_{1_{xx}}}{s_0}|_{\beta=s_1=s_2=0} = \frac{21}{5}B_2 + B_6,\\
2T^p_{11_s} &= \frac{-\varepsilon_{1_{xx}}}{s_1}|_{\beta=s_0=s_2=0} = \frac{21}{5}B_3 + B_7,\\
2T^p_{12_s} &= \frac{-\varepsilon_{1_{xx}}}{s_2}|_{\beta=s_0=s_1=0} = \frac{21}{5}B_4 + B_8,\\
2T_{2_s} &= \frac{-\varepsilon_{2_{xx}}}{\beta}|_{s_0=s_1=s_2=0}\\
&= \frac{1}{1-\phi}\left[1+\phi\frac{16-20\nu_0}{5}B_9\right] - \frac{\phi}{1-\phi}2T_{1_s},\\
2T^p_{20_s} &= \frac{-\varepsilon_{2_{xx}}}{s_0}|_{\beta=s_1=s_2=0}\\
&= \frac{\phi}{1-\phi}\frac{16-20\nu_0}{5}B_{10} - \frac{\phi}{1-\phi}2T^p_{10_s},\\
2T^p_{21_s} &= \frac{-\varepsilon_{2_{xx}}}{s_1}|_{\beta=s_0=s_2=0}\\
&= \frac{\phi}{1-\phi}\frac{16-20\nu_0}{5}B_{11} - \frac{\phi}{1-\phi}2T^p_{11_s},\\
2T^p_{22_s} &= \frac{-\varepsilon_{2_{xx}}}{s_2}|_{\beta=s_0=s_1=0}\\
&= \frac{\phi}{1-\phi}\frac{16-20\nu_0}{5}B_{12} - \frac{\phi}{1-\phi}2T^p_{12_s}.
\end{aligned}
\tag{38}
$$

Combining the two discussed boundary value problems, one obtains equations (37) and (38) that allow the elastic and inelastic interaction tensors to be computed; in turn, these are utilized in micromechanics schemes, such as the Mori–Tanaka and self-consistent schemes.

6. Mean field approaches for coated particulate or fiber composites

The computation of the interaction tensors, as described in the previous sections, is the first step toward identifying the macroscopic response of composite materials through the so-called mean field approaches.

Figure 4 illustrates a unidirectional fiber (or particulate) composite. This is the simplest type of composite that one can work with using the mean field methods. More complicated forms of microstructure include various types of reinforcement or oriented reinforcement in more than one direction (for instance, randomly oriented fibers).

All mean field micromechanics techniques treat the homogenization problem by considering each phase individually with its own volume fraction. For unidirectional coated fibers or particles inside a matrix, there are overall three phases: the matrix with elasticity tensor $\boldsymbol{L}_0$, constant eigenstrain ε_0^p, and volume fraction c_0; the fiber or particle with elasticity tensor $\boldsymbol{L}_1$, constant eigenstrain ε_1^p, and volume fraction c_1; and the coating layer with elasticity tensor $\boldsymbol{L}_2$, constant eigenstrain ε_2^p, and volume fraction c_2. Using the fraction ϕ between the fiber and the fiber–coating system, defined in the previous sections, one can easily show that

$$
c_2 = \frac{c_1}{\phi} - c_1, \qquad c_0 = 1 - \frac{c_1}{\phi}.
$$

The average microscopic strain at each phase is denoted ε_q, $q = 0, 1, 2$. The macroscopic strain ε and the macroscopic stress $\bar{\boldsymbol{\sigma}}$ are given by the expressions

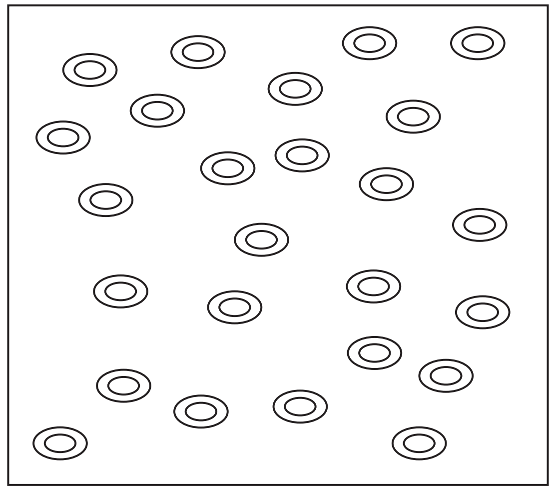

Figure 4. Unidirectional ellipsoidal particulate composite.

$$\bar{\varepsilon} = c_0\varepsilon_0 + c_1\varepsilon_1 + c_2\varepsilon_2,$$

$$\bar{\boldsymbol{\sigma}} = c_0\boldsymbol{\sigma}_0 + c_1\boldsymbol{\sigma}_1 + c_2\boldsymbol{\sigma}_2 \tag{39}$$

$$= c_0\boldsymbol{L}_0 : \left[\varepsilon_0 - \varepsilon_0^p\right] + c_1\boldsymbol{L}_1 : \left[\varepsilon_1 - \varepsilon_1^p\right] + c_2\boldsymbol{L}_2 : \left[\varepsilon_2 - \varepsilon_2^p\right]. \tag{40}$$

In principle, there are two goals that micromechanics methods seek to achieve: the first is to identify the macroscopic properties of the composite structure for known geometrical and material characteristics of the microstructure (homogenization problem). In mathematical terms, one aims to correlate the macroscopic quantities with a global relation of the form

$$\bar{\boldsymbol{\sigma}} = \bar{\boldsymbol{L}} : [\bar{\varepsilon} - \bar{\varepsilon}^p], \tag{41}$$

where $\bar{\boldsymbol{L}}$ is the macroscopic elasticity modulus and $\bar{\varepsilon}^p$ is the macroscopic eigenstrain. The second goal is to link the microscopic fields of the microstructural constituents with the macroscopic fields (localization problem), which are more easily obtained through direct experiments on the composite structure. This goal is served with the introduction of appropriate concentration tensors, which provide the connection between average microscopic and macroscopic strain fields. The scope of all mean field methods is the identification of average concentration tensors per phase.

The most famous mean field methods in micromechanics of random media are the Mori–Tanaka and the self-consistent strategies. For coated unidirectional fiber composites, the computational strategy of the two methods is described as follows.

6.1. Mori–Tanaka method

The main hypothesis of the Mori–Tanaka method is that each fiber, individually, is seen as a heterogeneity embedded in the matrix material with properties $\boldsymbol{L}_0$. This matrix is subjected to the eigenstrain ε_0^p and, at the far field, is under the average matrix strain ε_0. In that sense, equation (4) is utilized directly and the interaction tensors $\boldsymbol{T}$ and $\boldsymbol{T}^p$ represent dilute concentration tensors: they connect the average strains of the inhomogeneity and the coating layer with the average strain in the matrix. Substituting equation (4) into equation (40) yields

$$\varepsilon_0 = \boldsymbol{A}_0 : \bar{\varepsilon} + \boldsymbol{A}_{00}^p : \varepsilon_0^p + \boldsymbol{A}_{01}^p : \varepsilon_1^p + \boldsymbol{A}_{02}^p : \varepsilon_2^p, \tag{42}$$

with

$$
\begin{aligned}
&\boldsymbol{A}_0 = \left[c_0\mathcal{I} + c_1\boldsymbol{T}_1 + c_2\boldsymbol{T}_2\right]^{-1},\\
&\boldsymbol{A}^p_{00} = -\boldsymbol{A}_0 : \left[c_1\boldsymbol{T}^p_{10} + c_2\boldsymbol{T}^p_{20}\right],\\
&\boldsymbol{A}^p_{01} = -\boldsymbol{A}_0 : \left[c_1\boldsymbol{T}^p_{11} + c_2\boldsymbol{T}^p_{21}\right],\\
&\boldsymbol{A}^p_{02} = -\boldsymbol{A}_0 : \left[c_1\boldsymbol{T}^p_{12} + c_2\boldsymbol{T}^p_{22}\right].
\end{aligned}
\tag{43}
$$

Substituting equation (42) into equation (4) gives

$$
\begin{aligned}
&\varepsilon_1 = \boldsymbol{A}_1 : \bar{\varepsilon}_1 + \boldsymbol{A}^p_{10} : \varepsilon^p_0 + \boldsymbol{A}^p_{11} : \varepsilon^p_1 + \boldsymbol{A}^p_{12} : \varepsilon^p_2,\\
&\varepsilon_2 = \boldsymbol{A}_2 : \bar{\varepsilon} + \boldsymbol{A}^p_{20} : \varepsilon^p_0 + \boldsymbol{A}^p_{21} : \varepsilon^p_1 + \boldsymbol{A}^p_{22} : \varepsilon^p_2,
\end{aligned}
\tag{44}
$$

with

$$
\begin{aligned}
&\boldsymbol{A}_1 = \boldsymbol{T}_1 : \boldsymbol{A}_0, \quad \boldsymbol{A}^p_{10} = \boldsymbol{T}_1 : \boldsymbol{A}^p_{00} + \boldsymbol{T}^p_{10},\\
&\boldsymbol{A}^p_{11} = \boldsymbol{T}_1 : \boldsymbol{A}^p_{01} + \boldsymbol{T}^p_{11}, \quad \boldsymbol{A}^p_{12} = \boldsymbol{T}_1 : \boldsymbol{A}^p_{02} + \boldsymbol{T}^p_{12},\\
&\boldsymbol{A}_2 = \boldsymbol{T}_2 : \boldsymbol{A}_0, \quad \boldsymbol{A}^p_{20} = \boldsymbol{T}_2 : \boldsymbol{A}^p_{00} + \boldsymbol{T}^p_{20},\\
&\boldsymbol{A}^p_{21} = \boldsymbol{T}_2 : \boldsymbol{A}^p_{01} + \boldsymbol{T}^p_{21}, \quad \boldsymbol{A}^p_{22} = \boldsymbol{T}_2 : \boldsymbol{A}^p_{02} + \boldsymbol{T}^p_{22}.
\end{aligned}
\tag{45}
$$

Finally, implementing equations (42) and (44) in equation (40) and comparing with equation (41) yields

$$
\begin{aligned}
&\bar{\boldsymbol{L}} = c_0\boldsymbol{L}_0 : \boldsymbol{A}_0 + c_1\boldsymbol{L}_1 : \boldsymbol{A}_1 + c_2\boldsymbol{L}_2 : \boldsymbol{A}_2,\\
&\bar{\varepsilon}^p = \boldsymbol{M}_0 : \varepsilon^p_0 + \boldsymbol{M}_1 : \varepsilon^p_1 + \boldsymbol{M}_2 : \varepsilon^p_2,
\end{aligned}
\tag{46}
$$

with

$$
\begin{aligned}
&\boldsymbol{M}_q = -\bar{\boldsymbol{L}}^{-1} : \widetilde{\boldsymbol{n}}_q, \qquad q = 0, 1, 2,\\
&\widetilde{\boldsymbol{n}}_0 = c_0\boldsymbol{L}_0 : \boldsymbol{A}^p_{00} + c_1\boldsymbol{L}_1 : \boldsymbol{A}^p_{10} + c_2\boldsymbol{L}_2 : \boldsymbol{A}^p_{20} - c_0\boldsymbol{L}_0,\\
&\widetilde{\boldsymbol{n}}_1 = c_0\boldsymbol{L}_0 : \boldsymbol{A}^p_{01} + c_1\boldsymbol{L}_1 : \boldsymbol{A}^p_{11} + c_2\boldsymbol{L}_2 : \boldsymbol{A}^p_{21} - c_1\boldsymbol{L}_1,\\
&\widetilde{\boldsymbol{n}}_2 = c_0\boldsymbol{L}_0 : \boldsymbol{A}^p_{02} + c_1\boldsymbol{L}_1 : \boldsymbol{A}^p_{12} + c_2\boldsymbol{L}_2 : \boldsymbol{A}^p_{22} - c_2\boldsymbol{L}_2.
\end{aligned}
\tag{47}
$$

6.2. Self-consistent method

The main hypothesis of the self-consistent method is that each fiber, individually, is seen as a heterogeneity embedded in the effective medium with properties $\bar{\boldsymbol{L}}$. This medium is subjected to the eigenstrain ε^p and, at the far field, is under the average matrix strain ε. In that sense, one should substitute in equation (4) the properties and fields of phase 0 with those of the effective (unknown) homogenized material. Moreover, the interaction tensors $\boldsymbol{T}$ and $\boldsymbol{T}^p$ represent the concentration tensors: they connect the average strains of the inhomogeneity and the coating layer with the macroscopic strain,

$$
\begin{aligned}
&\varepsilon_1 = \bar{\boldsymbol{T}}_1 : \bar{\varepsilon} + \bar{\boldsymbol{T}}^p_{11} : \varepsilon^p_1 + \bar{\boldsymbol{T}}^p_{12} : \varepsilon^p_2 + \bar{\boldsymbol{T}}^p_{10} : \bar{\varepsilon}^p,\\
&\varepsilon_2 = \bar{\boldsymbol{T}}_2 : \bar{\varepsilon} + \bar{\boldsymbol{T}}^p_{21} : \varepsilon^p_1 + \bar{\boldsymbol{T}}^p_{22} : \varepsilon^p_2 + \bar{\boldsymbol{T}}^p_{20} : \bar{\varepsilon}^p.
\end{aligned}
\tag{48}
$$

The concentration tensors $\bar{\boldsymbol{T}}$ and $\bar{\boldsymbol{T}}^p$ are given by equation (15) for general ellipsoidal coated fibers, by equations (25), (26), (27), (28), and (29) for transversely isotropic coated long cylindrical fibers and by equations (36), (37), and (38) for isotropic coated spherical particles, when substituting $\boldsymbol{L}_0$ with $\bar{\boldsymbol{L}}$. This also implies that the Eshelby tensor $\boldsymbol{S}(\boldsymbol{L}_0)$ in equation (16) should be substituted with $\boldsymbol{S}(\bar{\boldsymbol{L}})$. Using equation (48) in equation (40) yields

$$
\varepsilon_0 = \bar{\boldsymbol{T}}_0 : \bar{\varepsilon} + \bar{\boldsymbol{T}}^p_{01} : \varepsilon^p_1 + \bar{\boldsymbol{T}}^p_{02} : \varepsilon^p_2 + \bar{\boldsymbol{T}}^p_{00} : \bar{\varepsilon}^p,
\tag{49}
$$

with

$$
\begin{aligned}
\overline{\boldsymbol{T}}_0 &= \frac{1}{c_0}\left[\mathcal{I} - c_1\overline{\boldsymbol{T}}_1 - c_2\overline{\boldsymbol{T}}_2\right],\\
\overline{\boldsymbol{T}}^p_{01} &= -\frac{1}{c_0}\left[c_1\overline{\boldsymbol{T}}^p_{11} + c_2\overline{\boldsymbol{T}}^p_{21}\right],\\
\overline{\boldsymbol{T}}^p_{02} &= -\frac{1}{c_0}\left[c_1\overline{\boldsymbol{T}}^p_{12} + c_2\overline{\boldsymbol{T}}^p_{22}\right],\\
\overline{\boldsymbol{T}}^p_{00} &= -\frac{1}{c_0}\left[c_1\overline{\boldsymbol{T}}^p_{10} + c_2\overline{\boldsymbol{T}}^p_{20}\right].
\end{aligned}
\tag{50}
$$

Combining equation (40) with equation (41), after some algebra, one obtains

$$
\begin{aligned}
\overline{\boldsymbol{L}} &= \boldsymbol{L}_0 + c_1[\boldsymbol{L}_1 - \boldsymbol{L}_0] : \overline{\boldsymbol{T}}_1 + c_2[\boldsymbol{L}_2 - \boldsymbol{L}_0] : \overline{\boldsymbol{T}}_2,\\
\overline{\varepsilon}^p &= \boldsymbol{M}_0 : \varepsilon^p_0 + \boldsymbol{M}_1 : \varepsilon^p_1 + \boldsymbol{M}_2 : \varepsilon^p_2,
\end{aligned}
\tag{51}
$$

with

$$
\boldsymbol{M}_q = -\left[\overline{\boldsymbol{L}} + c_1[\boldsymbol{L}_1 - \boldsymbol{L}_0] : \overline{\boldsymbol{T}}^p_{10} + c_2[\boldsymbol{L}_2 - \boldsymbol{L}_0] : \boldsymbol{T}^p_{20}\right]^{-1} : \widetilde{\boldsymbol{n}}_q,
\tag{52}
$$

for $q = 0, 1, 2$ and

$$
\begin{aligned}
\widetilde{\boldsymbol{n}}_0 &= -c_0\boldsymbol{L}_0,\\
\widetilde{\boldsymbol{n}}_1 &= -c_1\boldsymbol{L}_1 + c_1[\boldsymbol{L}_1 - \boldsymbol{L}_0] : \overline{\boldsymbol{T}}^p_{11} + c_2[\boldsymbol{L}_2 - \boldsymbol{L}_0] : \overline{\boldsymbol{T}}^p_{21},\\
\widetilde{\boldsymbol{n}}_2 &= -c_2\boldsymbol{L}_2 + c_1[\boldsymbol{L}_1 - \boldsymbol{L}_0] : \overline{\boldsymbol{T}}^p_{12} + c_2[\boldsymbol{L}_2 - \boldsymbol{L}_0] : \overline{\boldsymbol{T}}^p_{22}.
\end{aligned}
\tag{53}
$$

In addition, substituting equation (51) into equations (48) and (49) yields

$$
\begin{aligned}
\varepsilon_0 &= \boldsymbol{A}_0 : \overline{\varepsilon} + \boldsymbol{A}^p_{00} : \varepsilon^p_0 + \boldsymbol{A}^p_{01} : \varepsilon^p_1 + \boldsymbol{A}^p_{02} : \varepsilon^p_2,\\
\varepsilon_1 &= \boldsymbol{A}_1 : \overline{\varepsilon} + \boldsymbol{A}^p_{10} : \varepsilon^p_0 + \boldsymbol{A}^p_{11} : \varepsilon^p_1 + \boldsymbol{A}^p_{12} : \varepsilon^p_2,\\
\varepsilon_2 &= \boldsymbol{A}_2 : \overline{\varepsilon} + \boldsymbol{A}^p_{20} : \varepsilon^p_0 + \boldsymbol{A}^p_{21} : \varepsilon^p_1 + \boldsymbol{A}^p_{22} : \varepsilon^p_2,
\end{aligned}
\tag{54}
$$

where

$$
\begin{aligned}
\boldsymbol{A}_0 &= \overline{\boldsymbol{T}}_0, & \boldsymbol{A}^p_{01} &= \overline{\boldsymbol{T}}^p_{01} + \overline{\boldsymbol{T}}^p_{00} : \boldsymbol{M}_1,\\
\boldsymbol{A}^p_{00} &= \overline{\boldsymbol{T}}^p_{00} : \boldsymbol{M}_0, & \boldsymbol{A}^p_{02} &= \overline{\boldsymbol{T}}^p_{02} + \overline{\boldsymbol{T}}^p_{00} : \boldsymbol{M}_2,\\
\boldsymbol{A}_1 &= \overline{\boldsymbol{T}}_1, & \boldsymbol{A}^p_{11} &= \overline{\boldsymbol{T}}^p_{11} + \overline{\boldsymbol{T}}^p_{10} : \boldsymbol{M}_1,\\
\boldsymbol{A}^p_{10} &= \overline{\boldsymbol{T}}^p_{10} : \boldsymbol{M}_0, & \boldsymbol{A}^p_{12} &= \overline{\boldsymbol{T}}^p_{12} + \overline{\boldsymbol{T}}^p_{10} : \boldsymbol{M}_2,\\
\boldsymbol{A}_2 &= \overline{\boldsymbol{T}}_2, & \boldsymbol{A}^p_{21} &= \overline{\boldsymbol{T}}^p_{21} + \overline{\boldsymbol{T}}^p_{20} : \boldsymbol{M}_1,\\
\boldsymbol{A}^p_{20} &= \overline{\boldsymbol{T}}^p_{20} : \boldsymbol{M}_0, & \boldsymbol{A}^p_{22} &= \overline{\boldsymbol{T}}^p_{22} + \overline{\boldsymbol{T}}^p_{20} : \boldsymbol{M}_2.
\end{aligned}
\tag{55}
$$

7. Numerical examples

The interaction tensors of coated spherical particles and coated long cylindrical fibers are computed in the following examples with the help of the formulas presented in the three previous sections. For the numerical applications, Table 1 summarizes the material properties of the epoxy matrix, the glass inhomogeneity (particle or fiber) and the coating layer. All phases are isotropic. The ratio ϕ, expressed by equation (16), in the figures of this section varies from 0.5 (fiber and coating have the same content) to 0.99 (coating content is negligible).

7.1. Composites with coated long fibers

Figures 5, 6, 7, and 8 demonstrate several components of shear-related interaction tensors when the inhomogeneity is cylindrical long fiber. The two methods compared in these figures are the Berbenni

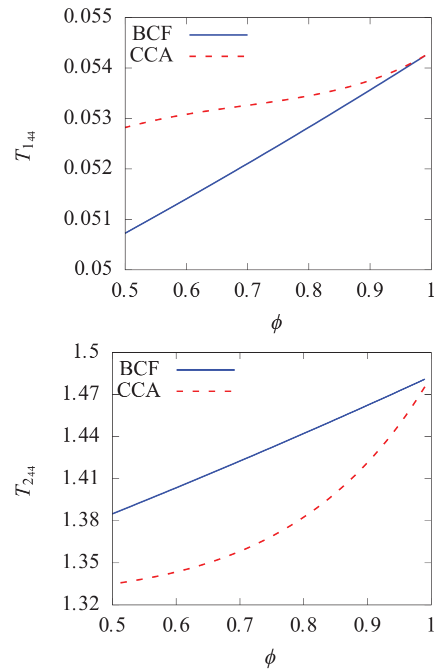

Figure 5. Elastic T_{44} components of interaction tensors: Berbenni and Cherkaoui [31] approach for fiber inhomogeneities (BCF) compared with composite cylinder assemblage (CCA).

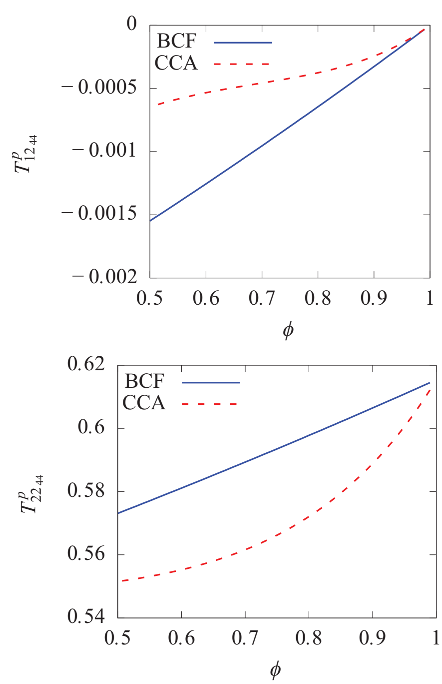

Figure 6. T^{p}_{44} components of interaction tensors related with the coating layer eigenstrains: Berbenni and Cherkaoui [31] approach for fiber inhomogeneities (BCF) compared with composite cylinder assemblage (CCA).

and Cherkaoui [31] approach (BCF) and the composite cylinder assemblage. From a theoretical point of view, the difference in the two methodologies arises only for the transverse shear term. In the case of transverse shear conditions, the strain inside the fiber is nonuniform, causing a slight error in the

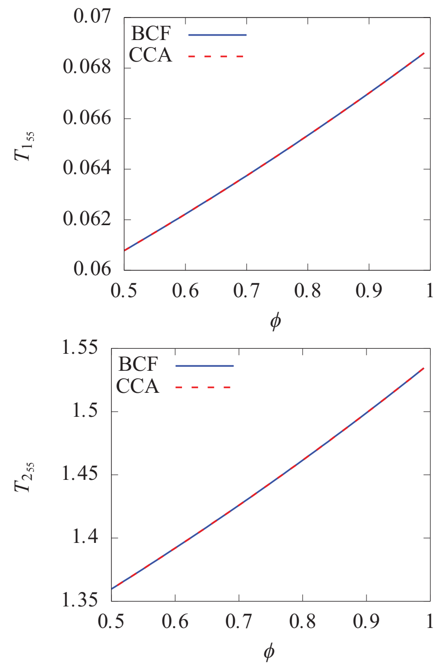

Figure 7. Elastic T_{55} components of interaction tensors: Berbenni and Cherkaoui [31] approach for fiber inhomogeneities (BCF) compared with composite cylinder assemblage (CCA).

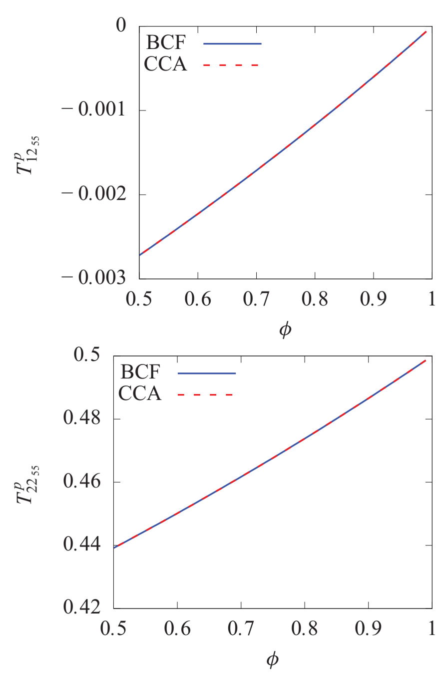

Figure 8. T^p_{55} components of interaction tensors related with the coating layer eigenstrains: Berbenni and Cherkaoui [31] approach for fiber inhomogeneities (BCF) for long cylindrical inhomogeneities compared with composite cylinder assemblage (CCA).

general relations (equation (15)). The affected terms are the components (1,1) and (4,4), while the components (1,3) and (5,5) coincide for all $\boldsymbol{T}$ and $\boldsymbol{T}^p$ tensors. As ϕ tends to 1 (i.e., the volume fraction of the coating layer tends to zero), the two methods render almost identical results in all terms.

Table 1. Material properties of epoxy matrix, glass inhomogeneity, and coating layer.

	E (GPa)	ν
Epoxy matrix	3	0.3
Glass inhomogeneity	81	0.25
Coating layer	2	0.35

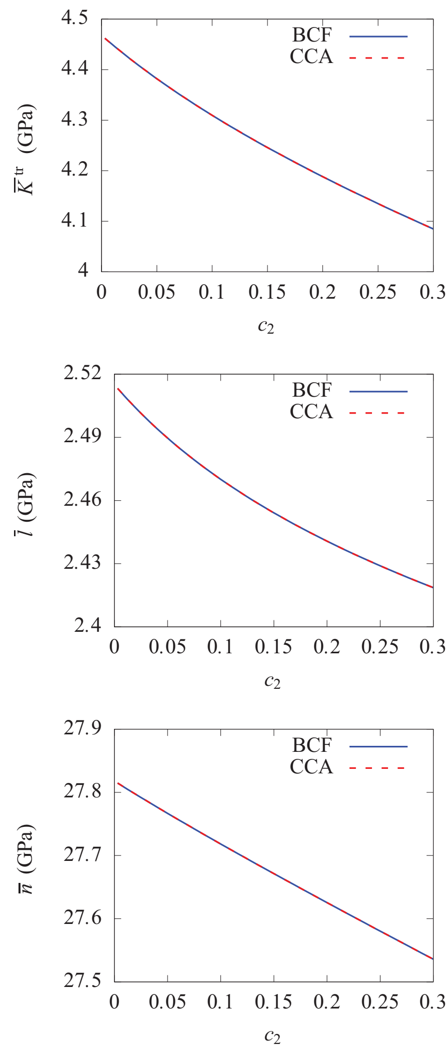

Figure 9. Predictions of macroscopic moduli for coated long cylindrical fiber composites: Berbenni and Cherkaoui [31] approach for fiber inhomogeneities (BCF) compared with composite cylinder assemblage (CCA).

Using the obtained interaction tensors, the Mori–Tanaka method is employed to obtain the macroscopic response of composites with coated long fibers. The material properties of the various phases are those presented in Table 1. The volume fraction of the fibers is fixed at 0.3 and the volume fraction of the coating layer varies from almost 0 to 0.3. Figures 9 and 10 show the predictions of the two approaches for the five macroscopic moduli. As expected, only the transverse shear modulus differs between the two methods. This difference is insignificant for a very small coating layer thickness.

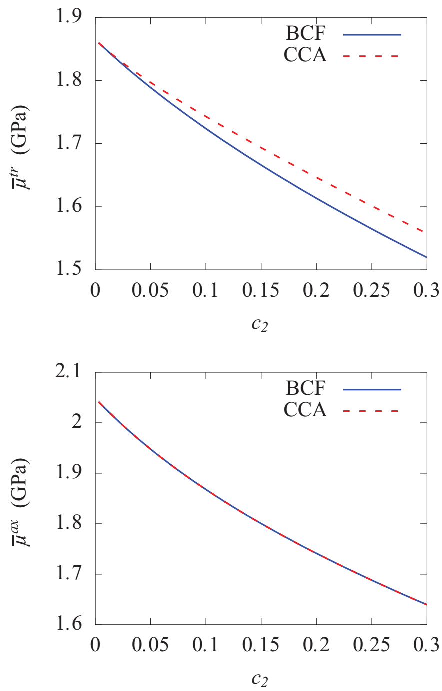

Figure 10. Predictions of macroscopic shear moduli for coated long cylindrical fiber composites: Berbenni and Cherkaoui [31] approach for fiber inhomogeneities (BCF) compared with composite cylinder assemblage (CCA).

7.2. Composites with coated spherical particles

Analogous conclusions are obtained for composites with coated spherical particles. In this case, the two compared methods are the Berbenni and Cherkaoui [31] approach (BCS) and the composite sphere assemblage. In terms of the interaction tensors, the difference between the two methodologies appears only in the shear components, where the strain inside the particle is nonuniform, causing a slight error in the general relations (equation (15)). Conversely, the bulk term of the interaction tensors is exactly the same for the two methods.

Considering the ratio ϕ to vary between 50% and 99%, the particle volume fraction equal to 30%, and the coating layer volume fraction to vary between almost 0 and 30%, the Mori–Tanaka method is employed to obtain the macroscopic response of composites with coated spherical particles. The material properties of the various phases are those presented in Table 1. Figure 11 illustrates the macroscopic properties predicted by the two methods. As expected, the bulk moduli coincide while the shear moduli differ between the two methods. The latter difference becomes insignificant for very small coating layer thicknesses.

With respect to the inelastic response, Figure 12 demonstrates the bulk and shear terms of the $\boldsymbol{M}_2$ tensor that connects the macroscopic eigenstrain with the eigenstrain at the coating layer, as equation (46) dictates. Again, the difference between the two approaches appears only in the shear term.

8. Conclusions

The scope of this manuscript was to discuss and compare micromechanics techniques aimed at describing the overall response of inelastic composites with coated reinforcement. This study can be very useful in developing proper semi-analytical multiscale schemes for nonlinear composites. Experimental observations have demonstrated that the interface between the matrix and the reinforcement is usually weak and behaves differently from the two material phases. Considering the interface as an additional material with its own properties can allow better identification of the composite's overall behavior.

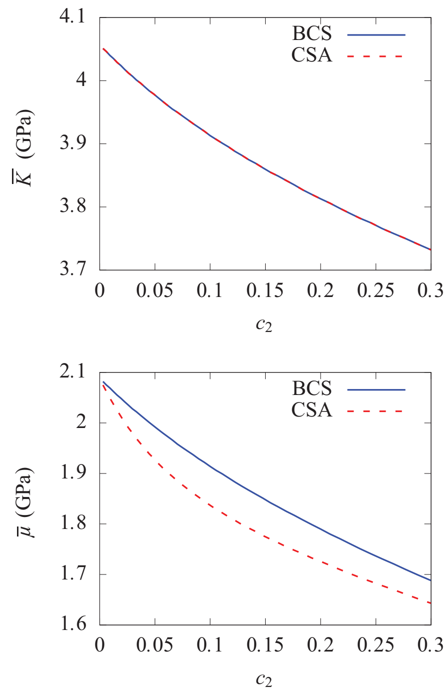

Figure 11. Predictions of macroscopic moduli for coated particulate composites: Berbenni and Cherkaoui [31] approach for spherical inhomogeneities (BCS) compared with composite sphere assemblage (CSA).

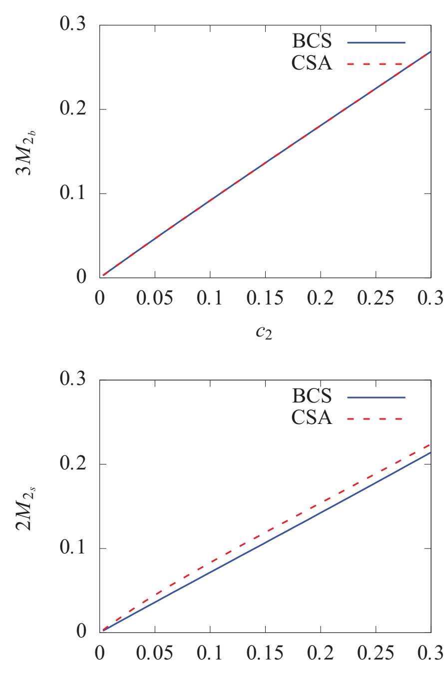

Figure 12. Bulk and shear component of the M_2 tensor, connecting the macroscopic and the coating layer eigenstrains: Berbenni and Cherkaoui [31] approach for spherical inhomogeneities (BCS) compared with composite sphere assemblage (CSA).

In this paper, Eshelby's inhomogeneity problem has been solved using a general methodology and two specific analytical techniques for infinitely long cylindrical fibers and spherical particles. Using this solution, the next step was to employ classical mean field methods, such as the Mori–Tanaka and self-consistent methods. Numerical simulations illustrated the comparison between the described methodologies.

From the studied numerical examples, it becomes evident that the Berbenni and Cherkaoui approach is quite accurate for small and moderate coating layer volume fractions. When large coating layer volume fractions are considered, it is more preferable to utilize more accurate techniques, such as the composite cylinder assemblage for coated long cylindrical fibers and the composite sphere assemblage for coated spherical particles. It is expected that these conclusions will also hold for the case of general ellipsoidal inhomogeneities. A proper validation of the general expressions (equation (15)) for short fibers should implicate other accurate techniques, such as, for instance, a full-field finite-element homogenization scheme.

Funding

This research received no specific grant from any funding agency in the public, commercial, or not-for-profit sectors.

Notes

1. Strictly speaking, the eigenstrains in inelastic mechanisms are generally nonuniform. A crucial assumption in mean field theories is that the inelastic strains or stresses are introduced per phase only with their average value [45], thus permitting the utilization of Eshelby's elastic problems. The accuracy of this hypothesis and the range of validity of the mean field approaches in inelastic problems has been extensively discussed in the literature [32].
2. The Voigt notation used in this section considers the following representation: 1, 2, and 3 denote the normal components along the directions r, θ, and z, respectively, while the shear components 4, 5, and 6 denote the terms in $r\theta$, rz, and θz, respectively.
3. For an infinitely long cylinder, $L \to \infty$. To avoid infinite values, the division by volume takes care of L.
4. The Voigt notation used in this section considers the following representation: 1, 2, and 3 denote the normal components at the directions r, θ, and φ, respectively, while the shear components 4, 5, and 6 denote the terms in $r\theta$, $r\varphi$, and $\theta\varphi$, respectively.

ORCID iD

George Chatzigeorgiou

References

[1] Kanouté, P, Boso, DP, Chaboche, JL, et al. Multiscale methods for composites: A review. *Arch Comput Methods Eng* 2009; 16: 31–75.
[2] Pindera, MJ, Khatam, H, Drago, AS, et al. Micromechanics of spatially uniform heterogeneous media: A critical review and emerging approaches. *Composites Part B* 2009; 40(5): 349–378.
[3] Geers, MGD, Kouznetsova, VG, and Brekelmans, WAM. Multi-scale computational homogenization: Trends and challenges. *J Comput Appl Math* 2010; 234(7): 2175–2182.
[4] Charalambakis, N, Chatzigeorgiou, G, Chemisky, Y, et al. Mathematical homogenization of inelastic dissipative materials: A survey and recent progress. *Continuum Mech Thermodyn* 2018; 30(1): 1–51.
[5] Mura, T. Micromechanics of defects in solids. In: *Mechanics of elastic and inelastic solids*, 2nd revised ed. Dordrecht: Kluwer Academic Publishers, 1987.
[6] Nemat-Nasser, S, and Hori, M. *Micromechanics: overall properties of heterogeneous materials*, 2nd ed. Amsterdam: North-Holland, 1999.
[7] Qu, J, and Cherkaoui, M. *Fundamentals of micromechanics of solids*. New Jersey: Wiley, 2006.
[8] Eshelby, JD. The determination of the elastic field of an ellipsoidal inclusion, and related problems. *Proc R Soc London, Ser A* 1957; 241(1226): 376–396.
[9] Ponte-Castañeda, P. The effective mechanical properties of nonlinear isotropic composites. *J Mech Phys Solids* 1991; 39: 45–71.
[10] Meraghni, F, and Benzeggagh, ML. Micromechanical modelling of matrix degradation in randomly oriented discontinuous-fibre composites. *Compos Sci Technol* 1995; 55(2): 171–186.
[11] Ponte-Castañeda, P, and Suquet, P. Nonlinear composites. *Adv Appl Mech* 1997; 34: 171–302.
[12] Fisher, FT, and Brinson, LC. Viscoelastic interphases in polymer-matrix composites: Theoretical models and finite-element analysis. *Compos Sci Technol* 2001; 61: 731–748.

[13] Desrumaux, F, Meraghni, F, and Benzeggagh, ML. Generalised Mori–Tanaka scheme to model anisotropic damage using numerical Eshelby tensor. *J Compos Mater* 2001; 35(7): 603–624.
[14] Meraghni, F, Desrumaux, F, and Benzeggagh, ML. Implementation of a constitutive micromechanical model for damage analysis in glass mat reinforced composite structures. *Compos Sci Technol* 2002; 62(16): 2087–2097.
[15] Doghri, I, and Ouaar, A. Homogenization of two-phase elasto-plastic composite materials and structures: Study of tangent operators, cyclic plasticity and numerical algorithms. *Int J Solids Struct* 2003; 40: 1681–1712.
[16] Chaboche, J, Kanoute, P, and Ross, A. On the capabilities of mean field approaches for the description of plasticity in metal matrix composites. *Int J Plast* 2005; 21: 1409–1434.
[17] Love, B, and Batra, RC. Determination of effective thermomechanical parameters of a mixture of two elastothermoviscoplastic constituents. *Int J Plast* 2006; 22: 1026–1061.
[18] Jendli, Z, Meraghni, F, Fitoussi, J, et al. Multi-scales modelling of dynamic behaviour for discontinuous fibre SMC composites. *Compos Sci Technol* 2009; 69(1): 97–103.
[19] Mercier, S, and Molinari, A. Homogenization of elastic-viscoplastic heterogeneous materials: Self-consistent and Mori–Tanaka schemes. *Int J Plast* 2009; 25: 1024–1048.
[20] Yvonnet, J, Gonzalez, D, and He, QC. Numerically explicit potentials for the homogenization of nonlinear elastic heterogeneous materials. *Comput Methods Appl Mech Eng* 2009; 198(33—36): 2723–2737.
[21] Tekoğlu, C, and Pardoen, T. A micromechanics based damage model for composite materials. *Int J Plast* 2010; 26: 549–569.
[22] Lahellec, N, and Suquet, P. Effective response and field statistics in elasto-plastic and elasto-viscoplastic composites under radial and non-radial loadings. *Int J Plast* 2013; 42: 1–30.
[23] Despringre, N, Chemisky, Y, Bonnay, K, et al. Micromechanical modeling of damage and load transfer in particulate composites with partially debonded interface. *Compos Struct* 2016; 155: 77–88.
[24] Anagnostou, D, Chatzigeorgiou, G, Chemisky, Y, et al. Hierarchical micromechanical modeling of the viscoelastic behavior coupled to damage in SMC and SMC-hybrid composites. *Composites Part B* 2018; 151: 8–24.
[25] Benveniste, Y, Dvorak, GJ, and Chen, T. Stress fields in composites with coated inclusions. *Mech Mater* 1989; 7: 305–317.
[26] Hori, M, and Nemat-Nasser, S. Double-inclusion model and overall moduli of multi-phase composites. *Mech Mater* 1993; 14: 189–206.
[27] Cherkaoui, M, Sabar, H, and Berveiller, M. Elastic composites with coated reinforcements: A micromechanical approach for nonhomothetic topology. *J Eng Mater Technol* 1995; 33(6): 829–843.
[28] Duan, HL, Yi, X, Huang, ZP, et al. A unified scheme for prediction of effective moduli of multiphase composites with interface effects. Part I: Theoretical framework. *Mech Mater* 2007; 39: 81–93.
[29] Wang, Z, Oelkers, RJ, Lee, KC, et al. Annular coated inclusion model and applications for polymer nanocomposites âã˜“ Part I: Spherical inclusions. *Mech Mater* 2016; 101: 107–184.
[30] Wang, Z, Oelkers, RJ, Lee, KC, et al. Annular coated inclusion model and applications for polymer nanocomposites—Part II: Cylindrical inclusions. *Mech Mater* 2016; 101: 50–60.
[31] Berbenni, S, and Cherkaoui, M. Homogenization of multicoated inclusion-reinforced linear elastic composites with eigenstrains: Application to thermoelastic behavior. *Philos Mag* 2010; 90(22): 3003–3026.
[32] Dvorak, G. Transformation field analysis of inelastic composite materials. *Proc R Soc London, Ser A* 1992; 437: 311–327.
[33] Dvorak, G, and Benveniste, Y. On transformation strains and uniform fields in multiphase elastic media. *Proc R Soc London, Ser A* 1992; 437: 291–310.
[34] Dvorak, G, Bahel-El-Din, Y, and Wafa, A. Implementation of the transformation field analysis for inelastic composite materials. *Comput Mech* 1994; 14: 201–228.
[35] Hashin, Z, and Rosen, BW. The elastic moduli of fiber-reinforced materials. *J Appl Mech* 1964; 31: 223–232.
[36] Hashin, Z. The elastic moduli of heterogeneous materials. *J Appl Mech* 1962; 29(1): 143–150.
[37] Chatzigeorgiou, G, Charalambakis, N, Chemisky, Y, et al. *Thermomechanical behavior of dissipative composite materials*. London: ISTE Press—Elsevier, 2018.
[38] Korringa, J. Theory of elastic constants of heterogeneous media. *J Math Phys* 1973; 14: 509–513.
[39] Walpole, LJ. A coated inclusion in an elastic medium. *Math Proc Cambridge Philos Soc* 1978; 83: 495–506.
[40] Hill, R. Interfacial operators in the mechanics of composite media. *J Mech Phys Solids* 1983; 31(4): 347–357.
[41] Cherkaoui, M, Sabar, H, and Berveiller, M. Micromechanical approach of the coated inclusion problem and applications to composite materials. *Int J Eng Sci* 1994; 116(3): 274–278.
[42] Hashin, Z. Thermoelastic properties of fiber composites with imperfect interface. *Mech Mater* 1990; 8: 333–348.
[43] Chatzigeorgiou, G, Seidel, GD, and Lagoudas, DC. Effective mechanical properties of aligned "fuzzy fiber" composites. *Composites Part B* 2012; 43: 2577–2593.
[44] Hashin, Z. Thermoelastic properties of particulate composites with imperfect interface. *J Mech Phys Solids* 1991; 39(6): 745–762.
[45] Lagoudas, DC, Gavazzi, AC, and Nigam, H. Elastoplastic behavior of metal matrix composites based on incremental plasticity and the Mori–Tanaka averaging scheme. *Comput Mech* 1991; 8: 193–203.